UCLouvain

École polytechnique de Louvain

Development of a Riemann problem for nonconservative product for plasmas in thermal non-equilibrium

Author: **Laurent Deleu**
Supervisors: **Thierry Magin, Philippe Chatelain**
Readers: **Miltiadis Papalexandris, Jean-François Remacle**
Academic year 2019–2020
Master [120] in Mechanical Engineering

Abstract

This thesis deals with the modelling of plasmas in thermal non-equilibrium and the numerical simulation of shocks. A simplified version of the multicomponent model, developed by [Graille&al], is presented where a nonconservative product term is found in the electron energy equation and represents an issue for the traditional conservative schemes. Among the introduced available solving strategies, a deeper focus is brought on a method that requires a decoupling of the system and that allows an analytical travelling wave solution for the electron variables. A numerical treatment of the nonconservative product, benefiting from this new approach and developed by [Wargnier&al], is then introduced. The contribution is divided into two parts: 1) an analysis of the impact on the physical validity of the solution that appears to violate the second principle of thermodynamics. 2) the rehabilitation of the two-temperatures relaxation process in the simplified model and its impact on the expression and the benefits of the aforementioned numerical treatment.

Acknowledgements

von KARMAN INSTITUTE FOR FLUID DYNAMICS

This master thesis was achieved in collaboration with the Von Karman Institute for Fluid Dynamics (Chaussée de Waterloo 72, 1640 Rhodes-Saint-Genèse, Belgium). Therefore, I would like to express my gratitude to this institute that allowed me to access its infrastructures. In particular, I would like to thank my main supervisor, Pr. Thierry Magin, who has supported me while I kept extending the submission date, for which I apologize.

I would also like to thank Dr. Bruno Dias for his patience when helping me install (three times) and familiarize with Stagline code, and for reviewing this report. Acknowledgements are also given to Pr. Philippe Chatelain and Pr. Tony Arts that helped me find this thesis topic. I would also like to thank Pr. Miltiadis Papalexandris and Pr. Grégoire Winckelmans who, thanks to their courses, orientate me towards the CFD domain. Finally, I would like to thank all the jury members that have accepted to evaluate my work.

To conclude this acknowledgements, I would like to thank my relatives for their support and more particularly Nathan Klavzer who helped me to improve the form quality of this manuscript.

Contents

Introduction

Still nowadays, plasmas are the topic of numerous researches as its applications can be found in various fields such as astrophysics, electric propulsion, atmospheric entry, and its modeling is more complex than the one of traditional fluids, due to its sensitivity to electromagnetism. The electrons and (partially or fully) ionized particles, that compose such matter, interact between one another through various phenomena. As far as collisions are concerned, while they normally help a classic fluid to thermalise, their effectiveness is, unfortunately, reduced here because of the mass disparity between the two aforementioned sets of particles. This will result into a thermal non-equilibrium that, added to a "multi-scale nature involving multiple spatial and temporal scales" (Wargnier [12]), requires specific models.

First approaches were provided with the use of multi-fluid models such as the one of Braginskii[2], that could already describe the thermal non-equilibrium thanks to a set of mass, momentum and energy conservation equations for each of the present species. However, this model was restricted to "high-temperature fully-ionised plasmas" only and could "lead to very stiff systems" (Wargnier[12]). A multi-component model, brought by Graille&al[1] removed such limitations. Based on a multi-scale analysis of plasmas, the model was derived from the Boltzmann equation (statistically dictating the velocity distribution in a fluid) using a Chapman-Enskog perturbative method. In the resulting governing equations, a non-conservative product term was noted in the electron energy equation.

Such a term introduced an issue when finding a numerical solution that makes use of methods based on the Riemann problem such as the Godunov scheme in the finite volume method context. Several approaches were proposed to fix this issue, starting with Dal Maso&al[7] proposing path-conservative schemes, though the corresponding solution is far from reality. This strategy was then improved by Chalons&Coquel[4] using modified cells. Two more popular methods were also proposed, consisting of retrieving the conservative term for the hyperbolic part of the system by either : 1) replacing the electron energy conservation equation by an entropy conservation equation Coquel&Marmignon[5] 2) treating the nonconservative product as a source term Candler&MacCormack[3]. Finally, a new approach was brought by Wargnier[12], benefiting from the literature in which " the temperature of the electrons is shown to be smooth whereas the temperature of the ions exhibits a discontinuity" and where it is shown that "the dissipative processes (...) depend on both the gradients of macroscopic quantities and the transport coefficients." (Wargnier[12]). The method suggests a decoupling of a simplified version of the system and develops regularized travelling wave solutions for the electrons as well as jump conditions close to reality. In that context, a numerical treatment of the nonconservative product was proposed and is proved to be effective for coarsely resolved meshes.

However, the decoupling approach, that involves removing the dissipative terms in one equation, relies on a commodity that "has no physical justification"(Wargnier[12]). The impact on physics of such a simplification is unknown, and therefore is the topic of the first part of the contribution of this thesis. Additionally, its second contribution aligns itself with the objective to generalize the numerical treatment to more complex systems. In that sense, the impact of the addition of a relaxation term to the decoupled system is studied. This manuscript is organised as follows:

Chapter 1: will introduce the atmospheric entry application, giving a context in which the contribution of this work could be used. A brief description of the main concepts of this thesis as well as the phenomena encountered during a meteor entry, will be provided. Finally, results from a simulation with "Stagline" code for a simplified test case, will be presented to give a first glance of the evolution of thermodynamic quantities through a shock.

Chapter 2: will summarise the development from the kinetics theory of the multi-component model (brought by Graille&al[1]) that will be dealt with. Assumptions that greatly simplifies the expressions and non-dimensional variables will first be introduced. After a short description of the kinetic derivation, the 0^{th} order of the Chapman-Enskog expansion will be detailed to finally obtain the reference couple system for this work. Additionally, the eigen structure of the hyperbolic part of the problem will be provided as well as an explanation of why the nonconservative product represents an issue.

Chapter 3: will present various approaches in order to solve the aforementioned coupled system. The focus will then be brought on the decoupling approach (brought by Wargnier[12]) and its elegant development of an analytical travelling wave solution. Eventually, its jump relations will be compared to the ones of other approaches as well as the ones of the coupled system obtained numerically.

Chapter 4: will be the continuation of the review of the work in [12]. The global scheme in the context of a finite volume method will be defined with its standard discretization of the nonconservative term. The limits of the latter will be shown for coarse meshes with respect to the diffusion length scale. A new specific treatment of the nonconservative product will then be developed, thanks to elements of the decoupling approach, and its benefits proved for under-resolved cases.

Chapter 5: will regard the first part of the contribution of this thesis. The physical validity of the travelling wave solution for the decoupled system will be evaluated with respect to the second principle of thermodynamics. In that sense, the entropy conservation equation will be obtained and its production term compared to the one of the coupled system. A phenomenon specific to the decoupled system solution will be presented, as well as a link with the entropy generation.

Chapter 6: will concern the second part of the contribution that consists of rehabilitating an energy exchange term in the electron energy equation. Its impact on the decoupled system and its solution will be studied for various orders of magnitude of the relaxation time constant. Moreover, an adaptation of the numerical treatment of the nonconservative term will be developed and its performances assessed for various resolutions with respect to the diffusion length.

Part I

State of the Art

Chapter 1

Atmospheric entry plasmas

The application of hypersonic atmospheric entry is the starting point by which the context of this thesis is introduced, since a bow-shock and plasma are present. Research is currently driven to better simulate the multiple phenomena involved and to improve the quality of the descent of space vehicles. This chapter helps to familiarise with the fundamental concepts of plasmas on which this work relies. Presented quantities will be more finely studied later on.

1.1 Plasma and shock waves

As a starting point, it is appropriate to give a short description of the two main physical concepts that govern this work.

Plasma : Meaning, in ancient Greek, "moldable substance", it is considered as the 4^{th} and most abundant fundamental state of matter. It can, indeed, be found in multiple applications such as storm lightning, neon lights, Earth's ionosphere/magnetosphere and stars. This form of matter stands out from the others by being partially or fully ionised, meaning that electrons can be separated from the original atom. Since these charges move freely, plasmas will be more inclined to have a strong response to electromagnetic field. All these particularities add complexity to models used to simulate the matter.

Shock wave : It is a moving pressure front that is viewed as a discontinuity from the point of view of continuum mechanics. Indeed, certain quantities will undergo a jump in their value over a non-zero, yet notably small distance, which is of the order of a few mean free paths of the molecules. Locally, the front can be normal or oblique to the flow field and can show some curvature on a larger scale, such as the bow shape in atmospheric entries. Considering the shock referential, velocities will always pass from supersonic to subsonic ($M_2 < 1 < M_1$) and there will always be a compression ($\frac{p_2}{p_1} > 1$) as they correspond to an increase in entropy abiding to the second principle of thermodynamics. Across the discontinuity, quantities will either jump or be conserved such as mass flow rate, total pressure, and total enthalpy (Hugoniot conditions). For a perfect gas, the following shock relations for pressure, density and temperature in terms of the upstream Mach number can be easily obtained :

$$\frac{p_2}{p_1} = \frac{\gamma M_1^2 - \frac{\gamma-1}{2}}{\frac{\gamma+1}{2}} \tag{1.1}$$

$$\frac{\rho_2}{\rho_1} = \frac{\frac{\gamma+1}{2} M_1^2}{1 + \frac{\gamma-1}{2} M_1^2} \tag{1.2}$$

$$\frac{T_2}{T_1} = \frac{(\gamma M_1^2 - \frac{\gamma-1}{2})}{\frac{\gamma+1}{2}} \frac{(1 + \frac{\gamma-1}{2} M_1^2)}{\gamma M_1^2 - \frac{\gamma-1}{2}}. \tag{1.3}$$

1.2 Governing equations based on a continuum approach

As for any other fluid, one can look for conservation laws that will locally rule the behaviour of the plasma. These result from more primary integral relations describing the balance of a certain quantity Φ. Basically, its temporal evolution on a fixed control volume Ω will be driven by fluxes f and volume sources/sinks Ψ, hence:

$$\frac{\partial}{\partial t}\int_{\Omega}\Phi(\mathbf{x},t)dv = \int_{\Omega}\nabla\cdot f(\Phi(\mathbf{x},t))dv + \int_{\Omega}\psi(\Phi(\mathbf{x},t)dv. \tag{1.4}$$

Getting rid of the integrals allows to obtain a local PDE but at the cost that several terms cannot be defined at a discontinuity. Special treatment must then be used for such a case as the differential form is not valid to capture a weak solution for the shock. However, working with this form remains valid outside the discontinuity. There can be several flux and source terms, each having their own expression that generally depends on Φ and that closes the problem. The following conservation equations from Scoggins[11] are presented with the intent to bring a quick overview of the contributions that appear in plasmas governing equations. However, the terms related to electromagnetism and radiation are not shown as they are neglected in the rest of this work.

Mass continuity: Considering S, the set of all species that can exist in a plasma, one could write a mass conservation equation for each k one of them leading to:

$$\frac{\partial}{\partial t}\rho_k + \nabla\cdot(\rho_k\mathbf{u}) + \nabla\cdot(\rho_k\mathbf{V_k}) = \dot{\omega}_k \qquad \forall k\in S. \tag{1.5}$$

The $\dot{\omega}_k$ source term accounts for the the chemical production. On the left side, two different fluxes are splitted, to put in evidence their respective advective and and diffusive origin. These could be added up to obtain a global flux for the species using $\mathbf{u}_k = \mathbf{u}+\mathbf{V}_k$, the species velocity being the sum of its diffusion velocity and the mass-averaged mixture velocity. Summing up the continuity equations of all species, the common total mass continuity equation is found:

$$\frac{\partial}{\partial t}\rho + \nabla\cdot(\rho\mathbf{u}) = 0, \tag{1.6}$$

where the chemical productions and the species velocities cancelled out between species.

Momentum conservation: Considering again the mass-averaged quantities, one has

$$\frac{\partial}{\partial t}(\rho\mathbf{u}) + \nabla\cdot(\rho\mathbf{u}\mathbf{u}) = -\nabla p + \nabla\cdot\underline{\mathbf{\Pi}}. \tag{1.7}$$

As in classical Navier-Stokes equations, the pressure and viscous stress tensor gradients are present.

Energy conservation: Here, the total energy $E = \frac{1}{\rho}\sum\rho_k e_k + \frac{1}{2}|\mathbf{u}|^2$ is considered, giving :

$$\frac{\partial}{\partial t}(\rho E) + \nabla\cdot(\rho H\mathbf{u}) = \nabla\cdot(\underline{\mathbf{\Pi}}\cdot\mathbf{u}) - \nabla q. \tag{1.8}$$

The same observations can be made as for the previous balance equation. Here, the flux terms merged into a term that corresponds to the convection of enthalpy $H = e + \frac{p}{\rho}$. Concerning the term ∇q, where q is the the charge of the mixture, it will vanish in the case of an electricaly quasi-neutral gas, i.e. ambipolar case.

Electrons energy conservation: In plasmas, free electrons are considered as a species on its own, like for every molecule and ion. However, the mass disparity ($m_e \ll m_h$) between them and heavier particles has a strong impact on the behaviour of the former. They will indeed have a higher thermal velocity leading to a "thermal non-equilibrium". Therefore, their internal energy is studied separately. Hence,

$$\frac{\partial}{\partial t}(\rho_e e_e) + \nabla \cdot (\rho h_e \mathbf{u}) = \mathbf{u} \cdot \nabla p_e - \nabla \cdot q_e + \Omega_e. \tag{1.9}$$

Here, the first term on the right side corresponds to the nonconservative product that will be discussed further on. Concerning the Ω_e term, it corresponds to energy exchange between electrons and heavy particles due to collisions (relaxation) or chemical reactions.

1.3 Atmospheric entries

It has been shown in the previous section that chemical (and radiation although not detailed) processes have an impact on the governing equations of a plasma. The application that is here considered, will illustrate phenomena that are at the origin of such terms in the context of an atmospheric entry that can concern either a spacecraft or a meteor. Regarding spacecrafts entries, they are the first part of an Entry-Descent-Landing sequence are responsible to reduce its kinetic and potential (with respect to the celestial body,i.e. Earth, surface) energies, dissipating them into thermal energy mainly through radiation and convection. A thermal protection system is present on the vehicle to handle the remaining conducted heat.

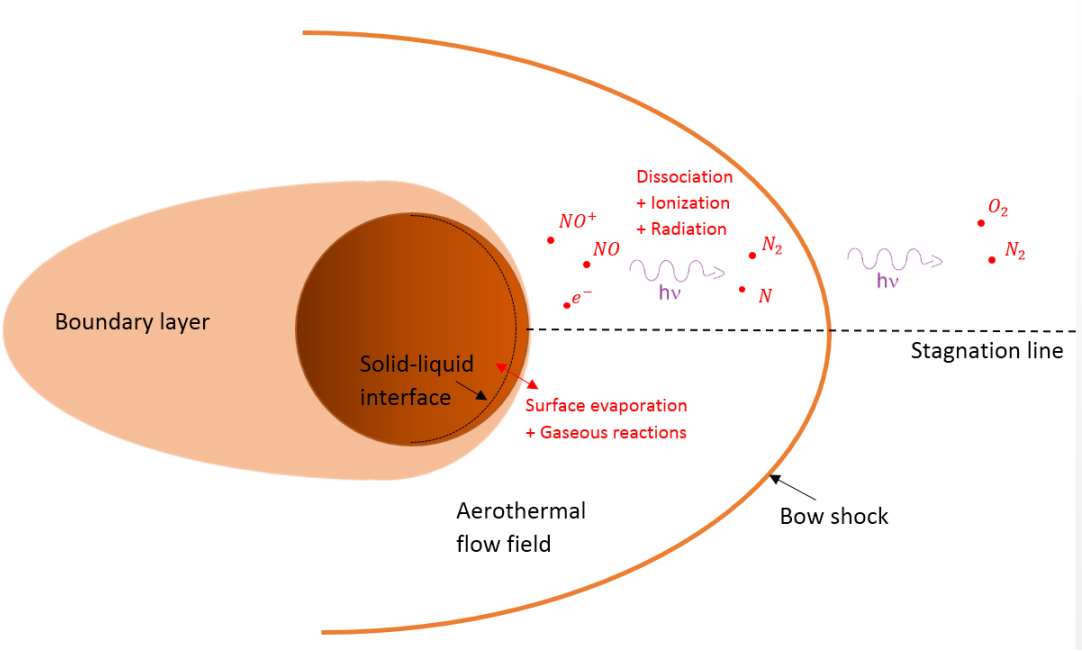

Figure 1.1: Chemistry around a meteor entry and stagnation line.

If the entering velocity of spacecrafts is often limited by the initial orbiting velocity, the one of entering meteors can be much bigger and reach $72km/s$ (according to Dias[**dias**]). Such a "hypersonic flight is characterised by velocity timescales comparable to chemical and kinetic timescales of the shocked gas" (Scoggins[11]). Indeed , the sudden temperature gain of the flow (sometimes from $270K$ in the freestream to $15,000K$ downstream) will induce multiple phenomena that are described in figure 1.1.

In the aerothermal flowfield that designates the area behind the bow shock, the high thermal energy is such that collisions between the gas molecules can now induce a dissociation, i.e. the

bond between two atoms breaks. Additional collisional excitation on these new radicals can lift their bound electrons to higher electronic states. Eventually, the electrons can be ripped of its atom, forming an ion and therefore plasma. In the case where an electron would drop to a lower energy state in its atom, this would provoke the emission of a photon that could then again initiate a reaction with other molecules, leading to photo-dissociation and photo-ionisation. Such reactions can even occur upstream of the shock meaning ions and free electrons can be found there.

As far as the meteor surface is concerned (although not the first preoccupation in this work) , various chemical reactions might take place depending on the composition of the body. The body progressively undergoes an ablation, meaning it loses mass from evaporation of its components (thanks to the heat brought by the flowfield) or from mechanical forces at the surface. Gaseous products are ejected in the boundary layer and wake in which chemistry can still take place. It can be noted that before evaporating, the body components sometimes melt, forming a liquid layer at the surface.

1.4 Stagnation line simulation

In the research around flowfields in front of a body in hypersonic case, a new approach was proposed by Klomfass[8]. It allows to go from a 2 axisymmetric formulation of the Navier-Stokes equations to a quasi one-dimensional one when just considering the stagnation streamline. The method includes a separation of variables as well as an ANSATZ, but developments won't be explained here as they go beyond the scope of this work. The reader can find additional details pertaining to this subject in [8]. The resulting equations called "Dimensionally Reduced Navier-Stokes Equations"(DRNSE) read as:

$$\frac{\partial}{\partial t}\mathbf{\Phi} + \frac{\partial}{\partial r}\mathbf{F^{inv}} + \frac{\partial}{\partial r}\mathbf{F^{vis}} + \frac{\mathbf{G^{inv}} + \mathbf{G^{vis}}}{r} = \mathbf{S^{c}}, \tag{1.10}$$

where $\mathbf{\Phi}$ denotes the volume-specific balance quantities vector, $\mathbf{F^{inv}}$ and $\mathbf{F^{vis}}$ are the inviscid and viscous flux vectors respectively, $\mathbf{G^{inv}}$ and $\mathbf{G^{vis}}$ are source terms arising from the development of the DRNSE, and $\mathbf{S^{c}}$ is an other source vector corresponding to chemistry. In [8] concluding remarks, the approach was described as "an ideal tool for the investigation of non-equilibrium and near local-equilibrium flows" although "only chemical non-equilibrium has been investigated". However, similar results were expected for thermal non-equilibrium.

This method is the one used in "Stagline" code developped by Munafo[10]. Coupled with the VKI physico-chemical "Mutation++" library (see Scoggins[11]), this code can simulate all phenomena that were previously presented using a broad range of possible flow mixtures. The spatial discretization is done by a finite volume method that can be chosen in the code options. In order to familiarise with the evolution of the involved physical quantities, a simulation was launched using a pure hydrogen mixture, neglecting chemical processes and using Roe's solver. The test case input parameters are gathered in table 1.1.

Boundary quantities	Values	Units
Upstream velocity u_∞	100,000	$[m/s]$
Upstream ρ_h	$4.039 \cdot 10^{-5}$	$[kg/m^3]$
Upstream ρ_e	$2.205 \cdot 10^{-8}$	$[kg/m^3]$
Upstream T_h	15,000	$[K]$
Upstream T_e	15,000	$[K]$
Wall temperature T_{wall}	10,000	$[K]$

Table 1.1: Input parameters for the presented Stagline test case.

Results are illustrated in figures 1.2, 1.3 and 1.4 where the surface of the meteor is located at $x = 0.1[m]$. The graphs generally confirm affirmations given earlier. Concerning the temperatures, they indeed reach their highest value in the flow field behind the shock. The thermal

boundary layer around the body can be observed, the curve eventually reaching the wall temperature value. It also appears that the shock relation seems different for electrons as it initially reaches a higher value before converging to the heavy particles temperature thanks to the relaxation phenomenon. Regarding the velocity results, an abrupt decrease is observed as expected, followed by a linear decrease before reaching a boundary layer that ends with the stagnation point. Finally, an inverted behaviour has also been observed for the pressure, although the sudden drop near the body surface is questionable. However, this won't be further discussed, as this work focuses on the shock only.

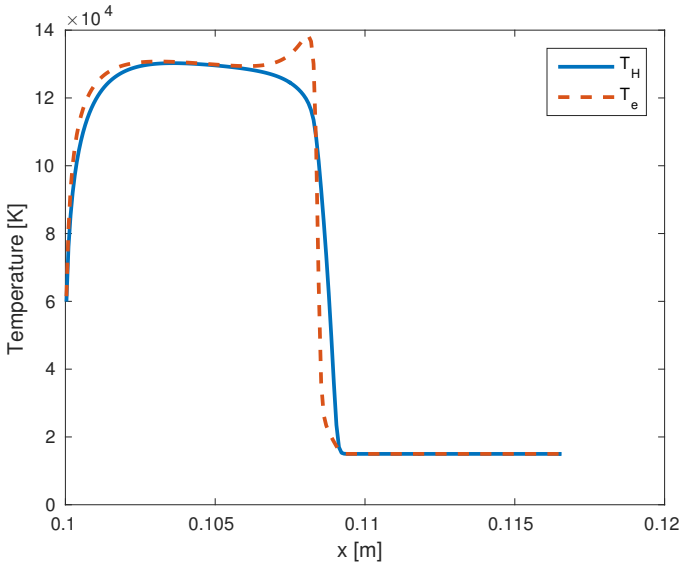

Figure 1.2: Species temperature evolution on a stagnation line.

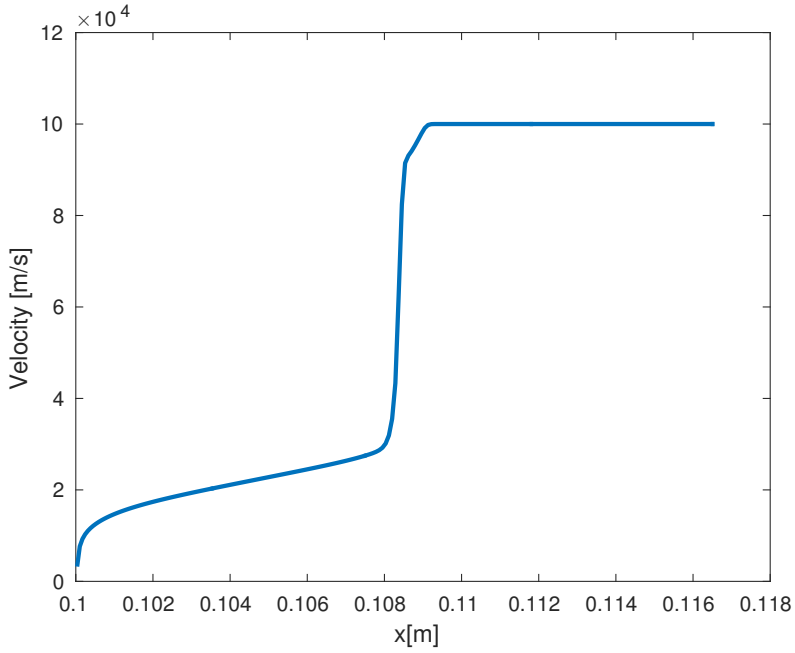

Figure 1.3: Flow field velocity evolution on a stagnation line.

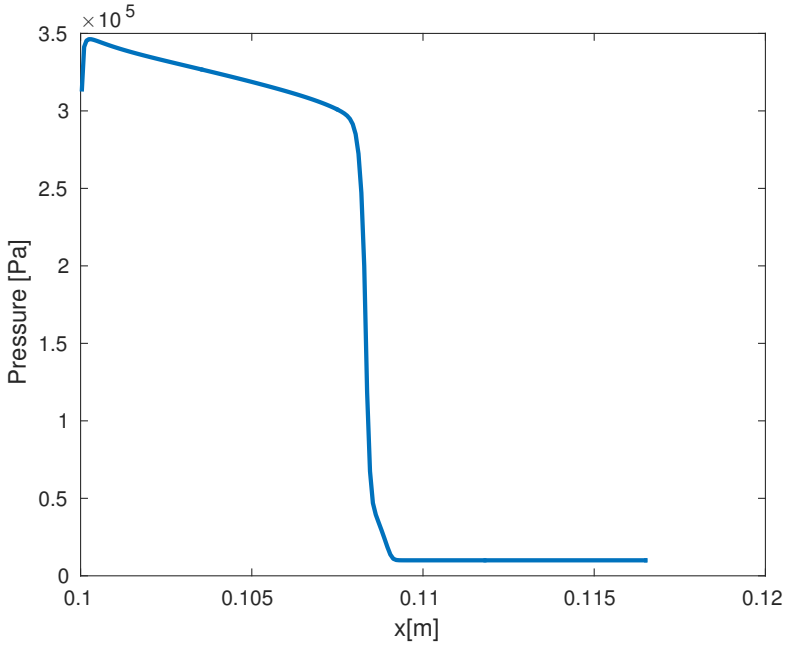

Figure 1.4: Pressure evolution on a stagnation line.

Chapter 2

Equation structure

In this chapter, the model for plasmas on which the rest of this work is based, will be introduced. Although a multifluid model could be used, the interest is brought on the multicomponent one developed, in Graille&al [1] , as the numerical treatment of the nonconservative product, proposed by Wargnier[12], takes its roots from there. The model is derived by a Chapman-Enskog expansion of the Boltzmann equation based on a multiscale analysis. A short description of the method will be presented as well as the resulting system of equations, its associated transport properties and its eigen structure. Finally, the issue, reltated to the appearance of a nonconservative term, will be presented.

Again, only a simplified case will be considered here. The following assumptions (as in [12]) are made:

- No chemistry,
- No electromagnetic forces,
- No Soret-Dufour effects,
- Isotropic and constant electron diffusion coefficient and thermal conductivity,
- Common adiabatic coefficient $\gamma = 5/3$ for both heavy particles and electrons.

2.1 Adimensionalisation

As it is done in [1] and [12], only nondimensional quantities will be dealt with. This is the occasion to introduce some of the macroscopic quantities that will be met later. Reference dimensional constants from table 2.1 will help to obtain their non-dimensional equivalents. Dimensional quantities are distinguished thanks to a *.

Starting with the space and time variables, they can be directly adimensionalised as:

$$x = \frac{x*}{L^0}, \qquad t = \frac{t^*}{t^0}.$$

Quantity	Notation
Macroscopic scale	L^0
Macroscopic timescale	t^0
Temperature	T^0
Number density	t^0
Electons mass	m_e^0
Characteristic heavy particles mass	m_h^0

Table 2.1: Dimensional reference quantities.

As all heavy particles will be considered together, there will be one number density accounting for the whole set. With the same quantity considered for the electrons, one can write:

$$n_h = \frac{n_h^*}{n^0}, \qquad n_e = \frac{n_e^*}{n^0}.$$

Regarding the density, a reference density can be expressed as a function of the number density for both sets:

$$\rho_h^0 = n^0 m_h^0, \qquad \rho_e^0 = n^0 m_e^0,$$

Allowing to not only remove the dimensions but also to find the following interesting relations :

$$\rho_h = \frac{\rho_h^*}{\rho^0} = \frac{n_h^* m_h^0}{n^0 m_h^0} = n_e, \qquad \rho_e = \frac{\rho_e^*}{\rho^0} = \frac{n_e^* m_e^0}{n^0 m_e^0} = n_e.$$

The treatment of the temperatures is straightforward :

$$T_h = \frac{T_h^*}{T_h^0}, \qquad T_e = \frac{T_e^*}{T_e^0}$$

Concerning the pressure, its reference can be expressed by a thermodynamic state relation with respect to Boltzmann constant and the previous reference constants as:

$$p^0 = n^0 k T^0.$$

Then, when performing as above :

$$p_h = \frac{p_h^*}{p^0}, \qquad p_e = \frac{p_e^*}{p^0}.$$

A total pressure can also be expressed through Dalton's law :

$$p = \frac{p^*}{p^0} = \frac{p_h^* + p_e^*}{p^0} = \frac{n_h^* k T_h^* + n_e^* k T_e^*}{n^0 k T^0} p_h = n_h k T_h + n_e k T_e.$$

As far as the thermal energy and the enthalpy are concerned, both will be divided by the same product. Hence, respectively,

$$e = \frac{e^*}{kT^0} = \frac{3}{2}T, \qquad h = \frac{h^*}{kT^0} = \frac{5}{2}T.$$

Finally, entropy, that will be studied further in the report, will be adimensionalised as :

$$s = \frac{s^*}{k}.$$

2.2 Kinetic derivation

The derivation of a model will now be summarised (more details available in [1]). The development starts at a microscopic level when defining a particle velocity distribution $f_i = f_i(\mathbf{x}, \mathbf{c}, t)$, in a six-dimensional state-space, that gives the probability of finding one particle at position $\mathbf{x}$, at velocity $\mathbf{c}$ and at time t.

The evolution in time is dictated by the (dimensional) Boltzmann equation that reads as:

$$\mathcal{D}_i^*(f_i^*) = \frac{\partial f_i^*}{\partial t^*} + \mathbf{c}^* \cdot \nabla_{x^*} f_i^* = \sum_j \mathcal{J}^*(f_i^*, f_j^*)$$

where $\mathcal{J}$ is the collision operator expressing the changes induced by the collisions with other species of the mixture. Up to now, the velocities were defined in a inertial referential in this

Order	Time	Heavy particles	Electrons
ε^{-2}	$t_{\mathfrak{e}}^0$		Thermalization $T_{\mathfrak{e}}$
ε^{-1}	$t_{\mathfrak{h}}^0$	Thermalization $T_{\mathfrak{h}}$	
ε^0	t^0	Euler Eqs.: ($M_{\mathfrak{h}}^{\varepsilon=0}$)	0^{th}-order drift-diffusion Eqs.: ($M_{\mathfrak{e}}^{\varepsilon=0}$)
ε	t^0/ε	Navier-Stokes Eqs.: ($M_{\mathfrak{h}}^{\varepsilon=1}$)	1^{st}-order drift-diffusion Eqs.: ($M_{\mathfrak{e}}^{\varepsilon=1}$)

Figure 2.1: Hierarchy of time scales for macroscopic equations from [1].

section. However, the above equation can be rewritten in a reference frame linked to the hydrodynamic velocity of the heavy particles $\mathbf{v}_h$, similarly to what is done in [1].
Now, two new nondimensional numbers are introduced:

$$\epsilon = \sqrt{\frac{m_e^0}{m_h^0}} \quad \text{and} \quad Kn = \frac{l^0}{L^0},$$

where l^0 is the mean free path. The former accounts for the mass disparity between heavy particles and electrons. The latter, called the "Knudsen number", generally helps to rewrite the Boltzmann equation into a dimensionless form. However, the present case allows to obtain a relation between these two parameters that appears to be of the same order of magnitude:

$$Kn = \frac{\epsilon}{M_h} \quad \text{where} \quad M_h = \frac{v_h^0}{V_h^0}$$

where M_h is the pseudo-Mach number and is order of one, and where V_h^0 is the heavy particles reference thermal speed. The Chapman-Enskog is then performed, consisting of writing the perturbed solution of the Boltzmann equation as a series using the parameter ϵ :

$$\begin{aligned} f_e &= f_e^0(1 + \epsilon\Phi_e + \epsilon^2\Phi_e^2 + \epsilon^3\Phi_e^3) + \mathcal{O}(\epsilon^4) \\ f_i &= f_i^0(1 + \epsilon\Phi_i + \epsilon^2\Phi_i^2) + \mathcal{O}(\epsilon^3) \end{aligned}$$

where Φ_e and Φ_i are perturbative functions. Injecting such an expression in the non dimensional Boltzmann equations, one obtains:

$$\epsilon^{-2}\mathcal{D}_e^{-2}(f_e^0)+\epsilon^{-1}\mathcal{D}_e^{-1}(f_e^0,\Phi_e)+\mathcal{D}_e^0(f_e^0,\Phi_e,\Phi_e^2)+\epsilon\mathcal{D}_e^1(f_e^0,\Phi_e,\Phi_e^2,\Phi_e^3) = \mathcal{J}_e^{-2}+\mathcal{J}_e^{-1}+\mathcal{J}_e^0+\mathcal{J}_e^1+\mathcal{O}(\epsilon^2),$$

and

$$\mathcal{D}_i^0(f_i^0) + \epsilon\mathcal{D}_e^1(f_i^0,\Phi_i) = \epsilon^{-1}\mathcal{J}_j^{-1} + \mathcal{J}_j^0 + \epsilon\mathcal{J}_j^1 + \mathcal{O}(\epsilon^2),$$

These terms correspond to the various powers of ϵ and can be separated to perform a multiscale analysis. Indeed, different processes will occur at different orders of the expansion. Table 2.1, taken from [1], summarises such phenomena. However, only the 0^{th} order expansion (third line of table 2.1) will be detailed here as it is the one that will be concerned in this thesis.

Governing equations : Macroscopic quantities can be expressed as a function of the velocity distribution function when integrating its product with a microscopic interpretation of the quantities. Here, the same principle is achieved after a projection on collisional invariants that account for the conservation of mass, momentum and kinetic energy at a microscopic level. The resulting equations for heavy particles read as:

$$\begin{cases} \partial_t\rho_i + \boldsymbol{\nabla}\cdot(\rho_i\mathbf{v}_h) = 0, \\ \partial_t(\rho_h\mathbf{v}_h) + \boldsymbol{\nabla}\cdot\left(\rho_h\mathbf{v}_h\mathbf{v}_h + \frac{1}{M_h^2}p\underline{\mathbf{I}}\right) = 0, \\ \partial_t(\rho_h e_h) + \boldsymbol{\nabla}\cdot(\rho_h e_h\mathbf{v}_h) = -p_h\boldsymbol{\nabla}\cdot\mathbf{v}_h + \Delta E_h^{(0)} \end{cases} \tag{2.1}$$

where $\Delta E_h^{(0)}$ is an energy transfer between electrons and heavy particles and where no diffusion term can be found as this order of the Chapman-Enskog expansion corresponds to the convective timescale. As far as the electrons conservation equations are concerned, one gets :

$$\begin{cases} \partial_t \rho_e + \boldsymbol{\nabla} \cdot \left[\rho_e \left(\mathbf{v}_h + \frac{1}{M_h} \mathbf{V}_e \right) \right] = 0, \\ \partial_t (\rho_e e_e) + \boldsymbol{\nabla} \cdot (\rho_e e_e \mathbf{v}_h) = -p_e \boldsymbol{\nabla} \cdot \mathbf{v}_h - \frac{1}{M_h} \boldsymbol{\nabla} \cdot \mathbf{q}_e + \Delta E_e^{(0)}. \end{cases} \tag{2.2}$$

where $\mathbf{V}_e$ is the electrons diffusion velocity, $\mathbf{q}_e$ is the electron heat flux and $\Delta E_e^{(0)}$ is a term that is the opposite of $\Delta E_h^{(0)}$. These are first-order drift diffusion equations whose fluxes will soon be expressed. Before, one new equation concerning the kinetic energy, is found by multiplying the mean heavy particles velocity, giving :

$$\partial_t \left(\frac{1}{2} \rho_h |\mathbf{v}_h|^2 \right) + \boldsymbol{\nabla} \cdot \left[\mathbf{v}_h \left(\frac{1}{2} \rho_h |\mathbf{v}_h|^2 + \frac{1}{M_h^2} p \right) \right] = \frac{1}{M_h^2} + p \boldsymbol{\nabla} \cdot \mathbf{v}_h. \tag{2.3}$$

Now introducing the total energy $\mathcal{E} = \rho_e e_e + \rho_h e_h + \frac{1}{2} \rho_h |\mathbf{v}_h|^2$ and the total enthalpy as $\mathcal{H} = \mathcal{E} + p$, one last conservation equation is found:

$$\partial_t \mathcal{E} + \boldsymbol{\nabla} \cdot (\mathcal{H} \mathbf{v}_h) = -\frac{1}{M_h} \boldsymbol{\nabla} \cdot \mathbf{q}_e \tag{2.4}$$

Transport properties : They designate the quantities that appear in the flux terms of the system and can be found by solving the first-order perturbation function Φ_e. To begin with, the first transport flux, the diffusion velocity, can be expressed as :

$$\mathbf{V}_e = -D \mathbf{d}_e - \frac{1}{T_e} \theta_e \boldsymbol{\nabla} T_e,$$

where $d_e = \frac{1}{p_e} \boldsymbol{\nabla} p_e$ is the driving force and D is the electron diffusion coefficient. The second transport flux is the heat flux :

$$\mathbf{q}_e = -\lambda \boldsymbol{\nabla} T_e - p_e \theta_e \mathbf{d}_e + \rho_e h_e \mathbf{q}_{\mathbf{e}e}$$

where λ is the electron thermal conductivity and h_e the electron enthalpy, already introduced in the previous section. Note that there is no transport proprieties corresponding to the heavy particles since they do not diffuse at such order of the expansion.

Relaxation : The last property that will be expressed is the energy exchange terms between heavy particles and electrons, caused by the elastic collisions. For the present order, their expressions read as:

$$\Delta E_h = \frac{\frac{3}{2} n_e (T_e - T_h)}{\tau}, \qquad \frac{1}{\tau_{he}} = \nu_{he} = \sum_j \frac{2 n_j}{3 n_e m_j} \nu_{je} \tag{2.5}$$

where τ_{he} is the average time between the collisions between the electron and another particle. Such a relaxation term "tends to relax the system towards a state of thermal equilibrium between the electrons and the heavy particles (...) Physically, if this characteristic collision time is small enough compared to the characteristic reference time, we have a thermal equilibrium state" (Wargnier [12])

2.3 Eigen structure

One should not consider all these energy equations as they are redundant. The final system, derived in the developments of the previous section, then reads as:

$$\begin{cases} \partial_t \rho_h + \boldsymbol{\nabla} \cdot (\rho_h \mathbf{v}_h) = 0, \\ \partial_t (\rho_h \mathbf{v}_h) + \boldsymbol{\nabla} \cdot (\rho_h \mathbf{v}_h \mathbf{v}_h + p\underline{\mathbf{I}}) = 0, \\ \partial_t \mathcal{E} + \boldsymbol{\nabla} \cdot (\mathcal{H}\mathbf{v}_h) = \boldsymbol{\nabla} \cdot (\lambda \boldsymbol{\nabla} T_e + \frac{5}{2} D \boldsymbol{\nabla} p_e) \\ \partial_t \rho_e + \boldsymbol{\nabla} \cdot (\rho_e \mathbf{v}_h) = \boldsymbol{\nabla} \cdot (\frac{1}{T_e} D \boldsymbol{\nabla} p_e), \\ \partial_t (\rho_e e_e) + \boldsymbol{\nabla} \cdot (\rho_e e_e \mathbf{v}_h) + p_e \boldsymbol{\nabla} \cdot \mathbf{v}_h = \boldsymbol{\nabla} \cdot (\lambda \boldsymbol{\nabla} T_e + \frac{5}{2} D \boldsymbol{\nabla} p_e). \end{cases} \tag{2.6}$$

where M_h is assumed to be equal to unity, where the relaxation term was neglected and where mass continuity equations of heavy particles were summed up. To better identify the nature of each term, the system of equations can be expressed as :

$$\partial_t \mathcal{U} + \boldsymbol{\nabla} \cdot \mathcal{F}(\mathcal{U}) + \boldsymbol{\nabla} \cdot \mathcal{N}(\mathcal{U}, \boldsymbol{\nabla}\mathcal{U}) = \mathcal{G}(\mathcal{U}, \boldsymbol{\nabla}\mathcal{U}) + \mathcal{S}(\mathcal{U}) \tag{2.7}$$

where the solution, convective fluxes, diffusive fluxes and nonconservative terms vectors are, respectively, defined as :

$$\mathcal{U} = (\rho_h, \rho_h \mathbf{v}_h, \mathcal{E}, \rho_e, \rho_e e_e)^T,$$

$$\mathcal{F}(\mathcal{U}) = (\rho_h \mathbf{v}_h, \rho_h \mathbf{v}_h \times \mathbf{v}_h, \mathcal{H}\mathbf{v}_h, \rho_e \mathbf{v}_h, \rho_e e_e \mathbf{v}_h)^T,$$

$$\mathcal{G}(\mathcal{U}, \boldsymbol{\nabla}\mathcal{U}) = \left(0, 0, \boldsymbol{\nabla} \cdot (\lambda \boldsymbol{\nabla} T_e + \frac{5}{2} D \boldsymbol{\nabla} p_e), \boldsymbol{\nabla} \cdot (\frac{1}{T_e} D \boldsymbol{\nabla} p_e), \boldsymbol{\nabla} \cdot (\lambda \boldsymbol{\nabla} T_e + \frac{5}{2} D \boldsymbol{\nabla} p_e) + \Delta E_e^{(0)}\right)^T,$$

$$\mathcal{N}(\mathcal{U}, \boldsymbol{\nabla}\mathcal{U}) = (0, 0, 0, 0, p_e \boldsymbol{\nabla} \cdot \mathbf{v}_h)^T.$$

The hyperbolic structure will now be given. Only considering the one-dimensional hyperbolic part of the system, one can write the system as:

$$\partial_t \mathcal{U} + A(\mathcal{U}) \boldsymbol{\nabla} \mathcal{U} = 0,$$

with :

$$A(\mathcal{U}) = \begin{pmatrix} 0 & 1 & 0 & 0 & 0 \\ \left(\frac{\gamma-3}{2}\right) |v_h|^2 & (3-\gamma) & \gamma - 1 & 0 & 0 \\ \left(\frac{\gamma-1}{2} v_h^2 - \frac{(H)}{\rho_h}\right) v_h & \left(\frac{(H)}{\rho_h} - \frac{\gamma-1}{2} |v_h|^2 - \right) & \gamma v_h & 0 & 0 \\ -\frac{\rho_e}{\rho_h} v_h & \frac{\rho_e}{\rho_h} & 0 & v_h & 0 \\ -\gamma \frac{\rho_e e_e}{\rho_h} v_h & \gamma \frac{\rho_e e_e}{\rho_h} & 0 & 0 & v_h \end{pmatrix}$$

The eigen values and their corresponding eigen vectors are the following :

$$\begin{aligned} \lambda_1 &= v_h - c & r_1 &= \left(1, v_h - c, \frac{H}{\rho_h} - v_h c, \frac{\rho_e}{\rho_h}, \gamma \frac{\rho_e e_e}{\rho_h}\right)^T \\ \lambda_2 &= v_h & r_2 &= \left(1, v_h - c, \frac{1}{2} v^2, 0, 0\right)^T \\ \lambda_3 &= v_h + c & r_3 &= \left(1, v_h + c, \frac{H}{\rho_h} + v_h c, \frac{\rho_e}{\rho_h}, \gamma \frac{\rho_e e_e}{\rho_h}\right)^T \\ \lambda_4 &= v_h & r_4 &= (0, 0, 0, 1, 0)^T \\ \lambda_5 &= v_h & r_5 &= (0, 0, 0, 0, 1)^T \end{aligned}$$

where the local sound speed is defined as $c = \sqrt{\gamma p / \rho_h}$. These eigen vectors vary only a little from the one that would have been obtained without the presence of the nonconservative product. When defining entropy as,

$$p_h = k \rho_h^\gamma exp(s_h / c_v) \quad \text{and} \quad p_e = k \rho_e^\gamma exp(s_e / c_v),$$

the following corresponding Riemann invariants are computed (from [6])

$$
\begin{array}{llll}
\beta_1^1 = s_h, & \beta_1^2 = \dfrac{v_h + 2c}{\gamma - 1}, & \beta_1^3 = \dfrac{\rho_h}{\rho_e}, & \beta_1^4 = \dfrac{\rho_h^\gamma}{\rho_e e_e}, \\
\beta_2^1 = v_h, & \beta_2^2 = p, & \beta_2^3 = \rho_e, & \beta_2^4 = \rho_e e_e, \\
\beta_3^1 = s_h, & \beta_3^2 = v_h - \dfrac{2c}{\gamma - 1}, & \beta_3^3 = \dfrac{\rho_h}{\rho_e}, & \beta_3^4 = \dfrac{\rho_h^\gamma}{\rho_e e_e}, \\
\beta_4^1 = \rho_h, & \beta_4^2, = \rho_h v_h, & \beta_4^3 = E, & \beta_4^4 = \rho_e e_e \\
\beta_5^1 = \rho_h, & \beta_5^2, = \rho_h v_h, & \beta_5^3 = E, & \beta_5^4 = \rho_e
\end{array}
$$

2.4 Non-conservative product issue

One may wonder what is the problem with the non-conservative product if an eigen structure can still be obtained and a solution to the Riemann problem can be found. The answer is the discretisation of the term in the context of trying to find a solution to this system numerically. For instance, when choosing the finite volume method, it will not be possible to benefit from such a structure as the nonconservative term cannot be put into a conservative form (i,e. into a divergence). Indeed, traditional schemes such as the Godunov method use the divergence theorem to be able to express the time evolution of a quantity in a volume as function of a sum of its fluxes evaluated at the interfaces. In order to find a numerical solution, one can still use these methods for the conservative part of the system but should use other tools for the non-conservative product, which is the topic of chapters 3 and 4.

Chapter 3

Solution approaches

Previously, the kinetic derivation of a model and its main non-conservative product issue were shown. Still, it is possible to elegantly obtain a numerical solution as presented in A. However, the strategy is not adapted for finite volumes schemes and, more particularly, Riemann problems. Other solution approaches for such a problem will now be presented with a deeper focus on the decoupling one that is the method assessed in this thesis.

3.1 Previous approaches

Through a 0^{th} order Chapman-Enskog expansion, the following system was derived:

$$\begin{cases} \partial_t \rho_h + \partial_x(\rho_h v_h) = 0 \\ \partial_t(\rho_h v_h) + \partial_x(\rho_h v_h^2 + p) = 0 \\ \partial_t \mathcal{E} + \partial_x(\mathcal{H} v_h) = \partial_x(\lambda \partial_x T_e + \frac{\gamma}{\gamma-1} D \partial_x p_e) \\ \partial_t \rho_e + \partial_x(\rho_e v_h) = \partial_x(D \frac{1}{T_e} \partial_x p_e) \\ \partial_t(\rho_e e_e) + \partial_x(\rho_e e_e v_h) + p_e \partial_x v_h = \partial_x(\lambda \partial_x T_e + \frac{\gamma}{\gamma-1} D \partial_x p_e). \end{cases} \tag{3.1}$$

Several methods to solve this system are available in the literature. For instance Chalons&Coquel[4] have proposed to change the common path-conservative schemes by introducing modified cells. However, here, only two approaches are presented: those of Coquel&Marmignon[5] and Candler&MacCormack[3]. Both strategies, focus on trying to recover a conservative form for system 3.1. The former replaces the electrons energy conservation equation by an entropy conservation equation that, in the a non diffusion case, reads as:

$$\partial_t(\rho_e s_e) + \partial_x \cdot (\rho_e s_e v_h) = 0.$$

The latter treats the non-conservative product $p_e \partial_x v_h$ as a source term, meaning that it is "moved" to the right side" and that a solution can be found considering the conservative part only. Again, when neglecting the diffusion terms, the last equation of system 3.1 is replaced by:

$$\partial_t(\rho_e e_e) + \partial_x(\rho_e e_e v_h) = 0.$$

Although the solutions of such systems are close to reality, their link with the original system has not been identified yet. However, their respective jump relations will be compared in what follows.

3.2 Decoupled system approach

Focus is now brought onto the approach proposed by Wargnier[12] which is a decoupling of system 3.1. This is obtained by removing the electrons diffusion terms in the total energy

conservation equation. The system is then split into a well known Euler system:

$$\begin{cases} \partial_t \rho_h + \partial_x(\rho_h v_h) = 0 \\ \partial_t(\rho_h v_h) + \partial_x(\rho_h v_h^2 + p) = 0 \\ \partial_t \mathcal{E} + \partial_x(\mathcal{H} v_h) = 0, \end{cases} \tag{3.2}$$

whose solution is a piecewise constant function for variables ρ_h, v_h, $\mathcal{E}$ and p where the discontinuity propagates at a σ speed found from Rankine-Hugoniot relations. Those will then be used to obtain a solution to the following nonconservative drift-diffusion system:

$$\begin{cases} \partial_t \rho_e + \partial_x \cdot (\rho_e v_h) = \partial_x(D \frac{1}{T_e} \partial_x p_e) \\ \partial_t(\rho_e e_e) + \partial_x(\rho_e e_e v_h) + p_e \partial_x v_h = \partial_x(\lambda \partial_x T_e + \frac{\gamma}{\gamma - 1} D \partial_x p_e). \end{cases} \tag{3.3}$$

The main advantage of this approach is that this second sub-system can provide an analytical solution for the electronic variables.

Travelling wave solution: The derivation of a solution for system 3.3 is now presented. To begin with, a change of spacial variable is performed, as the observer will now place itself in the shock referential. The piecewise constant functions resulting from the Euler system will only depend on $\xi = x - \sigma t$, the spatial coordinate that is function of the laboratory frame spatial coordinate x and the shock speed σ. This means they can be defined as :

$$\rho_h(\xi) = \begin{cases} \rho_h^L & \text{if } \xi < 0, \\ \rho_h^R & \text{if } \xi > 0, \end{cases} \qquad v_h(\xi) = \begin{cases} v_h^L & \text{if } \xi < 0, \\ v_h^R & \text{if } \xi > 0, \end{cases} \qquad p(\xi) = \begin{cases} p^L & \text{if } \xi < 0, \\ p^R & \text{if } \xi > 0, \end{cases}$$

where L and R denotes the upstream and downstream sides, respectively. As a piecewise travelling wave solution moving at the same speed σ , is sought for the electronic variables, it can be written that:

$$\begin{aligned} &\lim_{\xi \to -\infty} \rho_e(\xi) = \rho_e^L, \qquad \lim_{\xi \to \infty} \rho_e(\xi) = \rho_e^R, \qquad \lim_{\xi \to \pm\infty} = 0, \\ &\lim_{\xi \to -\infty} p_e(\xi) = p_e^L, \qquad \lim_{\xi \to \infty} p_e(\xi) = p_e^R, \qquad \lim_{\xi \to \pm\infty} = 0. \end{aligned}$$

Thus,states L and R electrons parameters are reached at an infinite distance behing and ahead of the shock, respectively. Applying the change of variable to system 3.3 and defining the total derivative as one with respect to variable ξ, one gets an ODE system:

$$\begin{cases} -\sigma \rho_e' + (\rho_e v_h)' = (D \frac{1}{T_e} p_e')' \\ -\frac{1}{\gamma - 1} \sigma (p_e)' + \frac{1}{\gamma - 1} (p_e v_h)' = -p_e v_h' + \lambda T_e'' + \frac{\gamma}{\gamma - 1} D p_e''. \end{cases} \tag{3.4}$$

The domain is then splitted in two and the positive ξ region is considered first. Integrating from $\xi = 0^+$ to $+\infty$, the following system is found.

$$\begin{pmatrix} p_e - p_e^R \\ T_e - T_e^R \end{pmatrix}' = \eta_R \begin{pmatrix} 1 & -\rho_e^R \\ -r^R \frac{\gamma - 1}{\gamma \rho_e^R} & r^R \end{pmatrix} \begin{pmatrix} p_e - p_e^R \\ T_e - T_e^R \end{pmatrix} \tag{3.5}$$

where thermal diffusivity and other right state constants are defined as

$$k^R = \frac{(\gamma - 1)\lambda}{\gamma \rho_e^R}, \qquad \eta^R = -\frac{c^R M_R}{D}, \qquad r^R = \frac{D}{k^R},$$

where the state R Mach number and speed of sound are introduced as:

$$M_R = \frac{\sigma - v_h^R}{c^R}, \qquad c^R = \sqrt{\gamma p^R / \rho_h^R}.$$

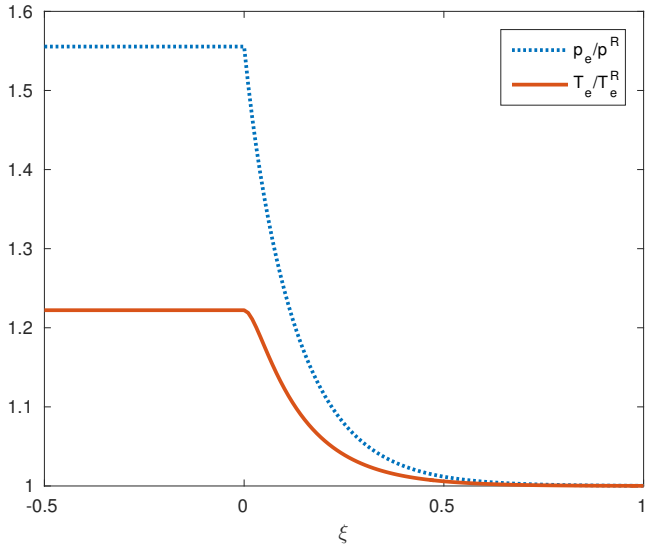

Figure 3.1: Travelling wave solution for electronic pressure and temperature for $M = 1.18$, $\rho_h^R = 1.0, \rho_e^R = 0.1$, $p_e^R = 0.1$ and $p_h^R = 1.0$ inputs.

In order to find an analytical solution, the eigen values of the square matrix in system 3.2, must first be expressed:

$$\delta^{\pm} = \frac{1}{2}\eta^R(1 + r^R \pm \sqrt{(1 + r^R)^2 - \frac{4}{\gamma}r)}).$$

A decomposition of the system in its eigen vectors can then be carried out, allowing to write the expression of the solution for the drift-diffusion system in terms of exponentials:

$$p_e(\xi) = p_e^R + \rho_e^R(K^{R+}e^{\delta^+\xi} + K^{R-}e^{\delta^-\xi}), \tag{3.6}$$

$$T_e(\xi) = T_e^R + (1 - \frac{\delta^+}{\eta^R})K^{R+}e^{\delta^+\xi} + (1 - \frac{\delta^-}{\eta^R})K^{R-}e^{\delta^-\xi}. \tag{3.7}$$

A similar expression is obtained for the negative ξ region replacing $K^{R\pm}$ by $K^{L\pm}$. The integration constants can be determined by ensuring that the solutions satisfy several conditions. To begin with, as the eigen values are strictly positive, $K^{L\pm}$ must be null as their corresponding exponential terms can only diverge. Regarding constants of the right state, they can be computed when imposing the continuity of the solution at $\xi = 0$ giving:

$$K^{R+} = \frac{2\eta^R T_e^R}{(\delta^- - \delta^+)} \frac{(M_R^2 - 1)\left(\frac{\gamma\delta^-}{\eta^R} - 1\right)}{(1-\gamma)M_R^2 + 2\gamma}$$

$$K^{R-} = \frac{2\eta^R T_e^R}{(\delta^- - \delta^+)} \frac{(M_R^2 - 1)\left(1 - \frac{\gamma\delta^+}{\eta^R}\right)}{(1-\gamma)M_R^2 + 2\gamma}.$$

Compatibility equations : These are relations that will play an important role in the numerical treatment of the nonconservative product detailed in the next chapter. They can be obtained by integrating the system from $\xi = 0^-$ to $\xi = 0^+$, and read as:

$$p_e(0)[v_h]_{(0)} = D[p_e']_{(0)}, \qquad [T_e']_{(0)} = 0. \tag{3.8}$$

A first observation is that the second relation dictates a continuity of the derivative of T_e, which is therefore null at $\xi = 0^+$ as observed on figure 3.1 where the analytical solution of the drift-diffusion system is shown. A second comment is that the discontinuity of the shock wave seems to depend on the dissipative process, as the pressure gradient jump is linked to the velocity jump and the diffusion coefficient D. This was already discussed in the literature as in Zel'dovich&Raizer [13].

3.3 Comparison of the jump conditions

Like in classical gas dynamics, one can find the jump conditions for the variables of interest. Regarding the Euler sub-system 3.2, p, ρ_h and T undergo jumps that can be expressed by relations 1.1. Additionally, new expressions can be obtained for the electrons[1] jump relations by integrating system 3.2 from 0+ to ∞, giving :

$$\frac{p_e^L}{p_e^R} = \frac{(\gamma+1)M_R^2}{(1-\gamma)M_R^2+2\gamma}, \qquad \frac{T_e^L}{T_e^R} = \frac{(\gamma-1)M_R^2+2}{(1-\gamma)M_R^2+2\gamma}, \qquad \frac{\rho_e^L}{\rho_e^R} = \frac{(\gamma+1)M_R^2}{(\gamma-1)M_R^2+2} \tag{3.9}$$

where it can be noted that the electric density jump is equivalent to the one of Rankine-Hugoniot.

Singularity : One could have already noticed that the denominators of the integration constants and of the p_e and T_e jump relations are equivalent and turn to zero for a certain $M_R = \sqrt{2\gamma/\gamma-1} \approx 2.24$. When reaching this critical Mach number, the constants diverge and the solution becomes invalid although, physically speaking, it is not the case. Therefore, the travelling wave solution has a region of validity close to 1.

Comparison with conventional jump conditions Comparing jump relations between different approaches is an easy way to assess their validity. Considering again the "entropy" and the "source" models introduced in section 3.1, those cases will have their own relations that, for the former, read as:

$$\frac{p_e^L}{p_e^R} = \left(\frac{(\gamma+1)M_R^2}{(\gamma-1)M_R^2+2}\right)^{\gamma}, \qquad \frac{T_e^L}{T_e^R} = \left(\frac{(\gamma+1)M_R^2}{(\gamma-1)M_R^2+2}\right)^{\gamma-1}, \qquad (\mathcal{M}_{ent})$$

and for the latter, give:

$$\frac{p_e^L}{p_e^R} = \frac{(\gamma+1)M_R^2}{(\gamma-1)M_R^2+2}, \qquad \frac{T_e^L}{T_e^R} = 1. \qquad (\mathcal{M}_{src})$$

The new model seems to better fit to the coupled case reference than the other approaches for Mach numbers close to unity, as seen in figure 3.3. Moreover,in opposition to other jump relations, the ones resulting from a decoupling overestimates the actual. However, the curve soon begins to diverge, as expected. These results suggest the validity of the decoupling method, albeit restricted to a certain range of Mach number.

[1] Jump relations can also be obtained for heavy particles variables

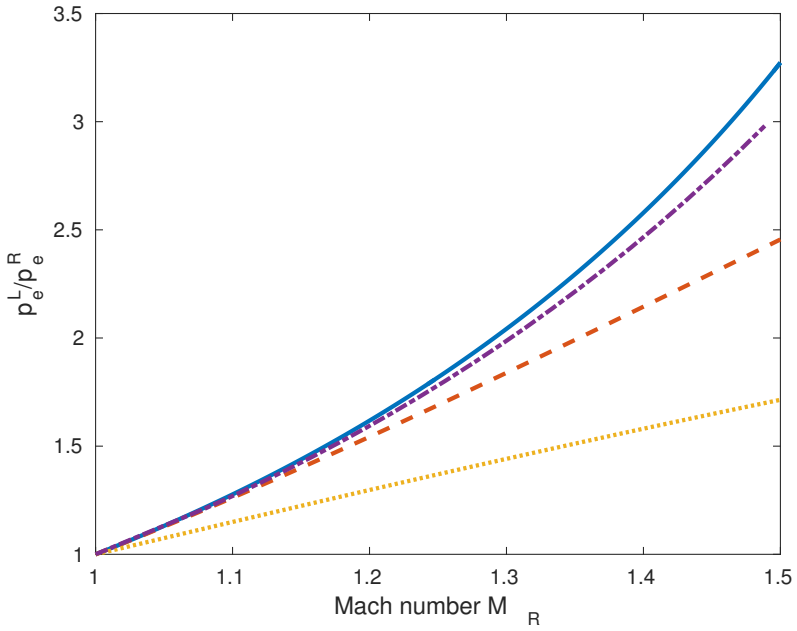

Figure 3.2: Evolution of pressure jump relation with the Mach number (travelling wave model in continuous line, coupled model in semi-dashed line, $\mathcal{M}_{ent}$ in dashed line and $\mathcal{M}_{src}$ in dotted line).

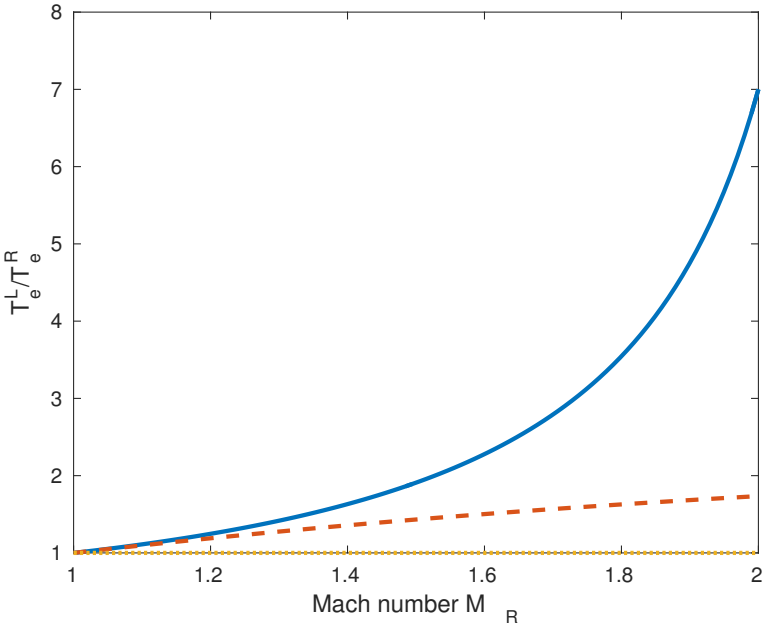

Figure 3.3: Evolution of temperature jump relation with the Mach number (travelling wave model in continuous line, $\mathcal{M}_{ent}$ in dashed line and $\mathcal{M}_{src}$ in dotted line).

Chapter 4

Numerical treatment of the nonconservative product

The decoupling approach has shown elegant results in the previous chapter, presenting a complete analytical solution consisting of a travelling wave and jump relations closer to reality than other methods, although it is restricted to Mach numbers close to unity. Nevertheless, Wargnier[12] showed that this can help to improve the strategy used to compute a numerical solution for the drift-diffusion system 3.3. The present chapter summarises the development and results of such a method that treats the problematic nonconservative product term.

4.1 Finite volume scheme

The numerical scheme takes the exact travelling wave solution as a initial condition that propagates with velocity σ. The latter, as well as state L quantities, can be determined from the state R ones, given as inputs. Dirichlet conditions are used at the boundaries of the finite domain where the derivatives are set to zero. The discretization is performed using a 1D finite Godunov method (see Leveque [9]) that can be an upwind or a Lax-Friedrichs scheme as "the proposed method to treat the nonconservative term is independent of the chosen finite volume scheme" (Wargnier[12]). Traditional cells are defined by the space step $\Delta x = L/N$ where L is the domain length and N the number of cells inside. Each cell $\mathcal{C}_j$ is centered at x_j and has its interfaces located at $x_{j\pm1/2}$. Once the time is also discretized in time steps Δt, the solution vector, which is the average of the numerical solution in the cell $\mathcal{C}_j$ at time t^n, can be introduced as:

$$U_j^n = (U_{j,1}^n, U_{j,2}^n) = (\rho_{e,j}^n, \rho_{e,j}^n e_{e,j}^n), \qquad \text{with} \quad n \geq 0, \quad 1 \leq j \leq N.$$

The sub-system 3.3 is then rewritten in a discretized manner, reading as:

$$U_j^{n+1} = U_j^n - \frac{\Delta t}{\Delta x}(F_{j+1/2}^n - F_{j-1/2}^n) + \frac{\Delta t}{\Delta x}(G_{j+1/2}^n - G_{j-1/2}^n) + N_j^n, \tag{4.1}$$

where $G_{j\pm1/2}^n$ and $F_{j\pm1/2}^n$ are diffusive and convective interface fluxes, respectively. The N_j^n vector, corresponding to the non-conservative product, should not be forgotten. A classical The upwind or Lax-Friedrichs scheme is used to compute the convective fluxes, solving a Riemann problem at each interface. Then, a second-order centered scheme is used to obtain the diffusive fluxes whose expression is:

$$G_{j+1/2}^n = \frac{1}{\Delta x}\left(D\frac{\gamma-1}{T_{e,j+1/2}^n}(U_{j+1,2}^n - U_{j,2}^n), \lambda(T_{e,j+1}^n - T_{e,j}^n) + D\gamma(U_{j+1,2}^n - U_{j,2}^n)\right) \tag{4.2}$$

where the electronic temperatures at a cell center and an interface, respectively, are defined as:

$$T_{e,j}^n = (\gamma-1)e_{e,j}^n = (\gamma-1)U_{j,2}^n/U_{j,1}^n$$
$$T_{e,j+1/2}^n = (T_{e,j+1}^n + T_{e,j}^n)/2.$$

Regarding the nonconservative term $N^n_{j,2}$, it is approximated as an integral on the volume $[x_{j-1/2}, x_{j+1/2}] \times [t^n, t^{n+1}]$ of its contribution in PDE system 3.3, that is:

$$N^n_{j,2} = \int_{t^n}^{t^{n+1}} \int_{x_{j-1/2}}^{x_{j+1/2}} p_e \partial_x v_h dx dt \simeq (\gamma - 1) U^n_{j,2} \int_{t^n}^{t^{n+1}} \int_{x_{j-1/2}}^{x_{j+1/2}} \partial_x v_h dx dt$$

where p_e is considered constant enough to be pulled out of the integral. Nevertheless, this approximation is consistent and can be called a 'standard' discretization.

4.2 Standard discretization results

The discretization, just presented above, is now assessed for different mesh qualities, i.e. fine or coarse meshes. As the length of the domain and the number of nodes are fixed to $L = 10$ and $N = 2000$, respectively, the resolution will be modified by changing the electron diffusion coefficient. Indeed, it is related to its corresponding diffusion length $L_D = D/[v_h]_{(0)}$, meaning that if it decreases, the mesh refinement might not be able to properly catch the motion, making the mesh coarse. Concerning the time discretization, it is dictated by a Fourrier condition $\Delta t \leq \frac{1}{2}\beta \Delta x^2$ with a Fourrier number being the maximum between D and thermal diffusion coefficient k^R.

	p	p_e	ρ_e	ρ_h	v_h	M
State R	1	0.1	0.01	1	0.2	1.183
State L	1.5	0.156	0.0127	1.274	0.527	0.856

Table 4.1: Test case parameters used in [12] and in following chapters.

Two extreme cases were selected : one over-resolved (OR) with 10^{-1} and one under-resolved with 10^{-3}. An electron thermal conductivity $\lambda = 0.001$ and state R inputs from the test case given in table 4.1, were used to numerically obtain[1] the shock curves (figure **??**) at t=1.

It appears that the maximum error of the over-resolved case, with respect to the exact curve, exceeds its under-resolved case equivalent by around 2 orders of magnitudes. The cause of such a difference would be a too small number of nodes N_D in the length L_D leading to two contributions of the problem: one "upstream of the shock due to numerical dissipation in the regular part of the travelling wave" and one "downstream of the shock due to the error on the gradients in the discontinuity" (Wargnier[12]) as depicted in figure 4.3. A numerical artefact is created because the continuity of T'_e is no longer respected.

Figure 4.4 depicts the L_2-norm of the error curves regarding the electronic pressure in figure **??** but with varying D, hence resolution. Linear regressions were performed to show that the upstream and downstream curves change of behavior at approximately the same number of nodes in L_D, for which artificial jumps start to be detected. Therefore, the conditions for solving the wave are detected and they corresponds to a minimum mesh refinement that depends on diffusion. Moreover, it is observed that the norm decreases when the resolution of the wave is raised. Thus, this standard discretization proves to be consistent if a mesh that has enough nodes in the diffusion length, is used.

[1]The results, obtained in this section might differ from the ones presented in [12] though they were computed using the same python "pygodunov2eq" code

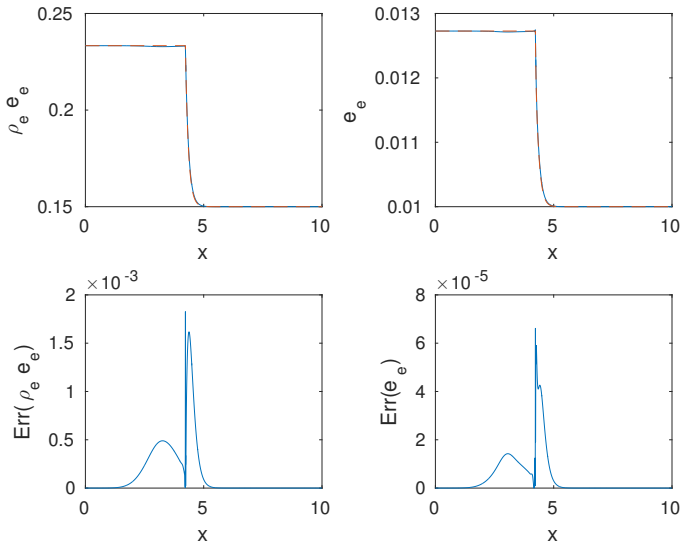

Figure 4.1: Over-resolved case. Electronic pressure and temperature (blue) sit on the 1^{st} line while errors with respect to the exact solution (dashed red) on the 2^{nd} line.

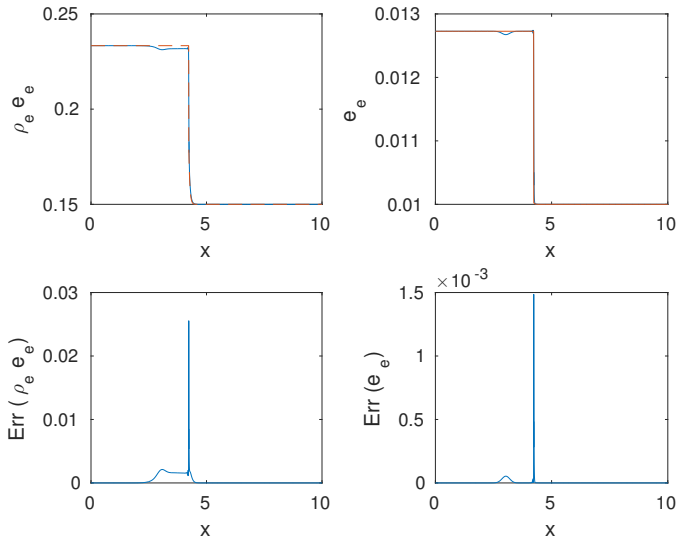

Figure 4.2: Under-resolved case. Electronic pressure and temperature (blue) sit on the 1^{st} line while errors with respect to the exact solution (dashed red) on the 2^{nd} line.

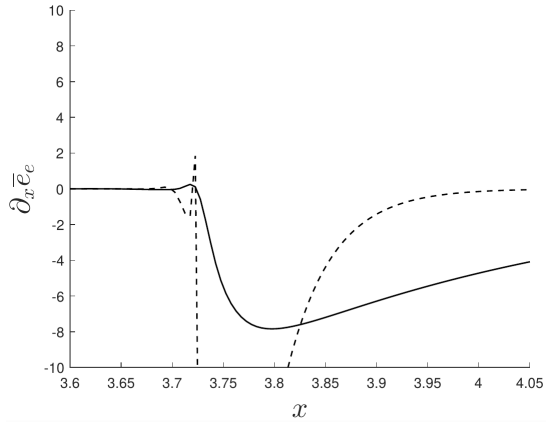

Figure 4.3: Quantity $\partial_x e_e$ for case OR (full line) and case UR (dashed line) at t=1. Image picked from [12]

.

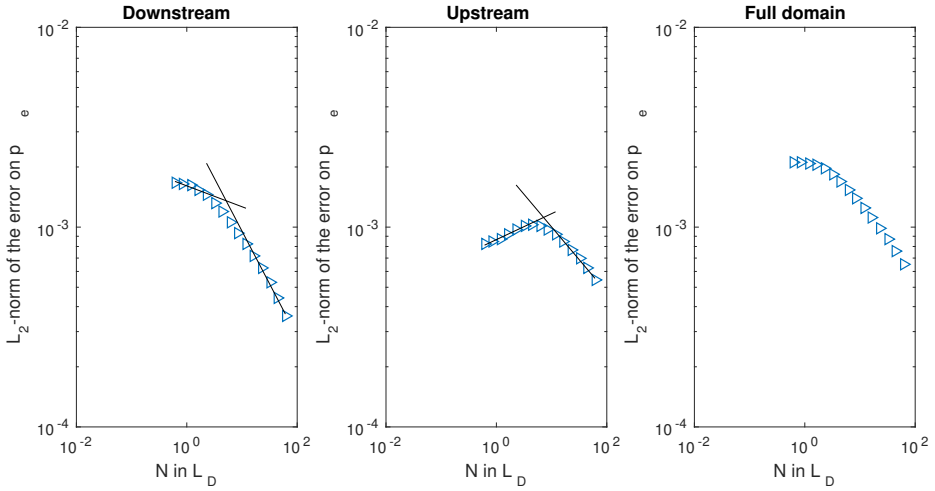

Figure 4.4: L_2-norm of the error on p_e with respect to the number of nodes in L_D. Downstream: slopes of the lines: 0.1045 and 0.5285. Upstream: slopes of the lines: -0.1299 and 0.3272.

4.3 Specific treatment of non conservative product

A first intuitive scheme for the nonconservative product was given above and proved to be consistent for well refined meshes only. Therefore, a new numerical treatment that works for coarser meshes as well, is needed. This was proposed by Wargnier[12], making use of the compatibility equations that he previously obtained (available in section 3.2). In this section, the developments and results of this discretization will be presented.

To begin with, the two lines (for each coordinate) of equation **??** are developed:

$$\begin{cases} U_{j,1}^{n+1} - U_{j,1}^{n} + \frac{\Delta t}{\Delta x}(F_{j+1/2,1}^{n} - F_{j-1/2,1}^{n}) = 0 + \frac{\Delta t}{\Delta x}(G_{j+1/2,1}^{n} - G_{j-1/2,1}^{n}) \\ U_{j,2}^{n+1} - U_{j,2}^{n} + \frac{\Delta t}{\Delta x}(F_{j+1/2,2}^{n} - F_{j-1/2,2}^{n}) = N_{j,2}^{n} + \frac{\Delta t}{\Delta x}(G_{j+1/2,2}^{n} - G_{j-1/2,2}^{n}). \end{cases} \tag{4.3}$$

Now, the second compatibility equation 3.2 from chapter 3 is discretized as:

$$T_{e,j+1}^{n} - T_{e,j}^{n} = T_{e,j}^{n} - T_{e,j-1}^{n} \quad \leftrightarrow \quad T_{e,j+1}^{n} - 2T_{e,j}^{n} + T_{e,j-1}^{n} = 0.$$

This allows to remove the thermal contribution in the diffusive flux term expressed in equation 4.1. The two coordinates can then be put in relation as:

$$G^n_{j\pm1/2,2} = \frac{\gamma}{\gamma-1} T^n_{e,j\pm1/2} G_{j\pm1/2,1}.$$

Then, multiplying the fist line of equation 4.3, subtracting it by the second line and neglecting the time derivatives, one can find a new expression for the nonconservative term:

$$\begin{aligned} N^n_{j,2} = &\frac{\Delta t}{\Delta x}(F^n_{j+1/2,2} - F^n_{j-1/2,2}) - \frac{\gamma}{\gamma-1} T^n_{e,j} \frac{\Delta t}{\Delta x}(F^n_{j+1/2,1} - F^n_{j-1/2,1}) \\ &- \frac{\Delta t}{\Delta x}(H^n_{j+1/2} - H^n_{j-1/2}), \end{aligned} \tag{4.4}$$

where the second-order terms read as:

$$H^n_{j\pm1/2} = \frac{\gamma}{2}(T^n_{e,j\pm1} - T^n_{e,j}) G^n_{j\pm1/2,1}.$$

Expression 6.2, thanks to its link with the compatibility equations, ensures the continuity of the derivative of the electrons temperature and the correct jump of the electrons pressure derivative. Consequently, this scheme should no longer be threatened by the appearance of an artificial jump due to a discontinuous temperature derivative at the discontinuity. However, it is also no longer consistent with the system, meaning additional terms must be added. Focusing only on first order terms, the correction can be found as the difference between the nonconservative product $-p_e \partial_x v_h$ and the limit of discretized expression 6.2 when Δx tends to zero. Finally, when discretising back the result and adding this correction, a final expression for the nonconservative term is obtained as:

$$\begin{aligned} N^{n*}_{j,2} = &\frac{\Delta t}{\Delta x}(F^n_{j+1/2,2} - F^n_{j-1/2,2}) - \frac{\gamma}{\gamma-1} T^n_{e,j} \frac{\Delta t}{\Delta x}(F^n_{j+1/2,1} - F^n_{j-1/2,1}) \\ &- \frac{\Delta t}{\Delta x}(H^n_{j+1/2} - H^n_{j-1/2}) \\ &- \Delta t v^n_{h,j} \frac{U^n_{j,2} - U^n_{j-1,2}}{\Delta x} + \frac{\gamma}{\gamma-1} \Delta t v^n_{h,j} U^n_{j,1} \frac{T^n_{e,j} - T^n_{e,j-1}}{\Delta x}. \end{aligned} \tag{4.5}$$

These additional terms could however lead to a non-validity of the compatibility equations. Therefore, these are limited by a certain ratio as "the dynamic of the wave is not depending on the choice of the cut-off" (Wargnier[12]).

The benefits of the new discretization are shown in figure 4.5 that compares the standard scheme and the new scheme with and without the correction terms for upstream, downstream and the total region. Indeed, the new scheme without correction terms starts to be inconsistent at a certain resolution level. As far as the case with correction terms is concerned, it exhibits better results at all scales. This achievement was made possible thanks to a good understanding of the travelling wave structure.

In [12], the results of an application to solar physics is provided, making use of a Strang splitting approach as well as diffusion substeps, reducing drastically the computational time, as the convective fluxes and the nonconservative term do not have to be computed each time the diffusion fluxes do (the Fourrier condition is often more restrictive than the CFL one). However, such an improvement to the scheme, won't be detailed in this state of the art as the contribution of this work focuses on the nonconservative product treatment in general.

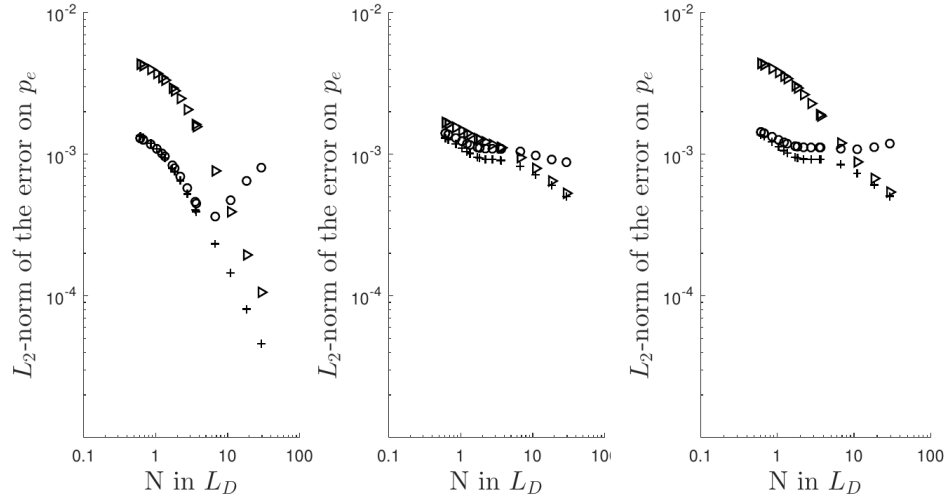

Figure 4.5: L_2-norm of the error on p_e with respect to the number of nodes in L_D, $\triangleright$ standard discretization, $\circ$ discretization without correction terms from eq (6.2), and $+$ discretization with correction terms from eq (4.3). Left: downstream domain contribution; middle: upstream domain contribution; right: full domain contribution. Image picked from [12]

Part II

Going further

Chapter 5

Physical validity of the decoupling approach

It was explained in chapter 3 how the validity of the travelling wave solution is limited to a range of Mach numbers close to unity. One may question the impact on physics of the decoupling approach with respect to the second law of thermodynamics. Hence, in this chapter, the focus resides on entropy, and more precisely, on the behaviour of internal entropy generation at the shock when the diffusion terms are dropped from the total energy conservation equation.

5.1 Entropy production for the coupled case

As for other quantities such as mass, momentum or total energy, a conservation law exists for entropy. The development used in this section to find this equation is the one proposed by Graille&al[1]. However, since the analysis is performed in the context of the system 3.1, the expressions will be significantly shorter. The initial step consists of choosing a relation where entropy appears, that is, the definition of Gibbs free energy :

$$g_e = h_e - T_e s_e, \qquad g_i = h_i - T_i s_i, \qquad i \in H. \tag{5.1}$$

Note that, initially, heavy particles are considered separately. Expressions are now needed for the Gibbs free energies and enthalpies. The following are selected:

$$\rho_e h_e = \frac{5}{2} n_e T_e, \qquad \rho_i h_i = \frac{5}{2} n_i T_i, \qquad i \in H,$$

and

$$\rho_e g_e = n_e T_e \ln\left(\frac{n_e n^0}{T_e^{3/2} Q_e^0}\right), \qquad \rho_i g_i = n_i T_i \ln\left(\frac{n_i n^0}{T_i^{3/2} Q_i^0}\right), \qquad i \in H,$$

where n^0, Q_e^0 and Q_i^0 are considered constant. Now using differential relations:

$$\rho_e \mathrm{d}\left(\frac{g_e}{T_e}\right) = \mathrm{d}n_e - \frac{3n_e}{2T_e}\mathrm{d}T_e, \qquad \rho_i \mathrm{d}\left(\frac{g_i}{T_h}\right) = \mathrm{d}n_i - \frac{3n_i}{2T_h}\mathrm{d}T_h, \qquad i \in H,$$

and definition 5.1, intermediate expressions for species entropy conservation are found:

$$\begin{aligned}
\partial_t(\rho_e s_e) + \boldsymbol{\nabla}\cdot(\rho_e s_e \mathbf{v_h}) &= \frac{1}{T_e}\left[\partial_t(\rho_e e_e) + \boldsymbol{\nabla}\cdot(\rho_e e_e \mathbf{v_h})\right] + n_e \boldsymbol{\nabla}\cdot\mathbf{v_h} \\
&\quad - \left[\partial_t \rho_e + \boldsymbol{\nabla}\cdot(\rho_e \mathbf{v_h})\right]\frac{g_e}{T_e}, \\
\partial_t(\rho_h s_h) + \boldsymbol{\nabla}\cdot(\rho_h s_h \mathbf{v_h}) &= \frac{1}{T_h}\left[\partial_t(\rho_h e_h) + \boldsymbol{\nabla}\cdot(\rho_h e_h \mathbf{v_h})\right] + n_h \boldsymbol{\nabla}\cdot\mathbf{v_h} \\
&\quad - \sum_{j\in H}\left[\partial_t \rho_j + \boldsymbol{\nabla}\cdot(\rho_j \mathbf{v_h})\right]\frac{g_j}{T_h}.
\end{aligned} \tag{5.2}$$

Finally, using the species mass and energy conservation equations found in 2 and new differential relations:

$$\mathrm{d}\left(\frac{g_e}{T_e}\right) = -\frac{h_e}{T_e^2}\mathrm{d}T_e + \frac{1}{p_e}\mathrm{d}p_e, \qquad \mathrm{d}\left(\frac{g_i}{T_h}\right) = -\frac{h_i}{T_h^2}\mathrm{d}T_h + \frac{1}{p_i}\mathrm{d}p_i, \qquad i \in H,$$

the seeked equation for the species entropy conservation is obtained:

$$\begin{aligned}\partial_t(\rho_e s_e) + \boldsymbol{\nabla}\cdot(\rho_e s_e \mathbf{v_h}) &= -\boldsymbol{\nabla}\cdot\frac{1}{T_e}(\mathbf{q_e} - \rho_e g_e \mathbf{V_e}) \\ &\quad - \frac{p_e}{T_e}\mathbf{d_e}\cdot\mathbf{V_e} - \frac{1}{T_e}\boldsymbol{\nabla}\ln T_e\cdot(\mathbf{q_e} + \rho_e h_e \mathbf{V_e}), \\ \partial_t(\rho_h s_h) + \boldsymbol{\nabla}\cdot(\rho_h s_h \mathbf{v_h}) &= 0. \end{aligned} \tag{5.3}$$

The absence of source terms and other flux terms other than pure convection is explained by the chosen context that is a 0^{th} order Chapman-Enskog expansion, meaning that only electrons have dissipative processes. A global entropy conservation equation is now obtained by summing up the contributions of electrons and heavy particles . Regrouping the terms into fluxes enables then to obtain one final compact expression :

$$\partial_t(\rho s) + \boldsymbol{\nabla}\cdot(\rho s \mathbf{v_h}) + \boldsymbol{\nabla}\cdot\boldsymbol{\mathcal{J}} = \Upsilon, \tag{5.4}$$

where the global entropy flux and source terms respectively read as

$$\begin{aligned}\boldsymbol{\mathcal{J}} = \boldsymbol{\mathcal{J}_e} &= \frac{1}{T_e}(\mathbf{q_e} - \rho_e g_e \mathbf{V_e}), \\ \Upsilon = \Upsilon_e &= -\frac{p_e}{T_e}\mathbf{d_e}\cdot\mathbf{V_e} - \frac{1}{T_e}\boldsymbol{\nabla}\ln T_e\cdot(\mathbf{q_e} + \rho_e h_e \mathbf{V_e}). \end{aligned} \tag{5.5}$$

Recalling that there are neither electromagnetic forces nor Soret-Dufour effects, the entropy production can finally be written as:

$$\Upsilon = \frac{D}{p_e T_e}\left|\boldsymbol{\nabla} p_e\right|^2 + \frac{\lambda}{T_e^2}\left|\boldsymbol{\nabla} T_e\right|^2. \tag{5.6}$$

This expression for entropy generation is directly determined as strictly positive, therefore respecting second law of thermodynamics.

5.2 Additional source terms for the decoupled case

It was shown that the entropy production could have a heavy particles contribution, though, turning out to be null in the previous particular case. Expressions for Υ_e and Υ_h were obtained using the corresponding mass and energy conservation. The decoupled system (3.2&3.3) case is now considered and its structural differences should impact expression 5.1. Here, the electrons dissipative processes are removed from the total energy equation, giving :

$$\partial_t(\mathcal{E}) + \boldsymbol{\nabla}\cdot(H\mathbf{v_h}) = 0. \tag{5.7}$$

However, dissipative terms remain in the electronic energy equation meaning that the heavy particle energy equation also changes considering $\mathcal{E} = \rho_h e_h + \rho_e e_e + \frac{1}{2}\rho_h\left|\mathbf{v}_h\right|^2$ and assuming constant kinetic energy [1]. A new equation for the heavy particles energy conservation is therefore obtained using this relation on $\mathcal{E}$ and definitions and conservation equations 2.2 + 5.2.

$$\begin{aligned}\partial_t(\rho_h e_h) + \boldsymbol{\nabla}\cdot(\rho_h e_h \mathbf{v_h}) &= \partial_t(\mathcal{E}) + \boldsymbol{\nabla}\cdot(H\mathbf{v_h}) - \partial_t(\rho_h e_h) + \boldsymbol{\nabla}\cdot(\rho_h e_h \mathbf{v_h}) \\ &\quad - \partial_t\left(\frac{1}{2}\rho_h\left|\mathbf{v}_h\right|^2\right) + \nabla\cdot\left[\mathbf{v}_h\left(\rho_h\left|\mathbf{v}_h\right|^2 + p\right)\right] \\ &= \boldsymbol{\nabla}\cdot\mathbf{q_e} + p_h\boldsymbol{\nabla}\cdot\mathbf{v_h}\end{aligned}$$

[1] Considering kinetic energy modified and heavy particles energy unchanged would give equivalent results

Following now the same methodology as in the previous section but with the above expression, a new equation for heavy particles entropy conservation is found:

$$\begin{aligned}\partial_t(\rho_h s_h) + \boldsymbol{\nabla}\cdot(\rho_h s_h \mathbf{v_h}) &= \frac{1}{T_h}\left[\partial_t(\rho_h e_h) + \boldsymbol{\nabla}\cdot(\rho_h e_h \mathbf{v_h})\right] + n_h \boldsymbol{\nabla}\cdot\mathbf{v_h} \\ &\quad - \sum_{j\in H}\left[\partial_t\rho_h + \boldsymbol{\nabla}\cdot(\rho_h\mathbf{v_h})\right]\frac{g_i}{T_h} \\ &= \frac{1}{T_h}\boldsymbol{\nabla}\cdot\mathbf{q_e} \\ &= -\frac{1}{T_h}\boldsymbol{\nabla}\cdot\left(\lambda\boldsymbol{\nabla}T_e + \frac{5}{2}D\boldsymbol{\nabla}p_e\right). \end{aligned} \tag{5.8}$$

The heavy particles entropy source term appears to be no longer null. Its expression is close to the one of electronic dissipative terms in the energy conservation equations. Moreover, the T_h denominator reminds the heavy particles origins and ensures entropy dimensions. Therefore, the overall entropy source term reads :

$$\Upsilon = \frac{D}{p_e T_e}\left|\boldsymbol{\nabla}p_e\right|^2 + \frac{\lambda}{T_e^2}\left|\boldsymbol{\nabla}T_e\right|^2 - \frac{1}{T_h}\boldsymbol{\nabla}\cdot\left(\lambda\boldsymbol{\nabla}T_e + \frac{5}{2}D\boldsymbol{\nabla}p_e\right), \tag{5.9}$$

an expression that can no longer be directly stated as positive.

5.3 Relation with the incoming Mach number

Knowing the analytical expressions for travelling waves p_e and T_e, it is possible to relate Υ and M_R. Beforehand, the entropy source term must be translated in 1D and in the wave referential, i.e. as function of $\xi = x - \sigma t$ as done in chapter 3. This leads to

$$\Upsilon(\xi) = \frac{D}{p_e(\xi)T_e(\xi)}(p_e'(\xi))^2 + \frac{\lambda}{T_e^2}(T_e'(\xi))^2 - \frac{\lambda}{T_h(\xi)}T_e''(\xi) - \frac{5}{2}\frac{D}{T_h(\xi)}p_e''(\xi).$$

As the focus is brought on the shock itself and not the surrounding region, the above function is evaluated at $\xi = 0^+$. Indeed, T_e and p_e gradients are not defined at $\xi = 0$ and null for $\xi = 0^-$. Using

$$\begin{aligned} p_e(0) &= p_e^L \\ T_e(0) &= T_e^L \\ T_e'(0) &= 0 \\ p_e'(0^+) &= \rho_e^R\left(K^{R+}\delta^+ + K^{R-}\delta^-\right) \\ p_e''(0^+) &= \rho_e^R\left(K^{R+}(\delta^+)^2 + K^{R-}(\delta^-)^2\right) \\ T_e''(0^+) &= \left(1 - \frac{\delta^+}{\eta^R}\right)K^{R+}(\delta^+)^2 + \left(1 - \frac{\delta^-}{\eta^R}\right)K^{R-}(\delta^-)^2, \end{aligned}$$

with eigen values and integration constants expressions,again, provided in chapter 3 and after several developments, the following analytical result is found:

$$\Upsilon(0^+) = \frac{2(\eta^R)^3(M_R^2-1)}{(\delta^- - \delta^+)((1-\gamma)M_R^2 + 2\gamma)}\left[\frac{((\delta^-)^2 + (\delta^+)^2)}{\eta^R(\delta^- + \delta^+)}f_1(M_R, ...) - \frac{\lambda T_e^R}{T_h}f_2(...) - \frac{5}{2}\frac{DP_e^R}{T_h}f_3(...)\right]$$

with

$$f_1 = \frac{2\eta^R(M_R^2-1)((1-\gamma)M_R^2+2\gamma)}{\eta^R\gamma(\gamma-1)(4M_R^4-8M_R^2+4)-(7\gamma^2+1)M_R^4-(2\gamma+2)^2M_R^2+2(3\gamma^2+4\gamma+3)}$$
$$f_2 = \frac{(\delta^+)^3-(\delta^-)^3}{(\eta^R)^3}+\frac{(\gamma\delta^+\delta^-+(\eta^R)^2)((\delta^-)^2-(\delta^+)^2)}{(\eta^R)^4}-\frac{\gamma\delta^+\delta^-(\delta^--\delta^+)}{(\eta^R)^3}$$
$$f_3 = \frac{\gamma\delta^+\delta^-(\delta^+-\delta^-)}{(\eta^R)^3}+\frac{(\delta^-)^2-(\delta^+)^2}{(\eta^R)^2}.$$

The dependence on M_R being removed from the eigenvalues by dividing them by η^R, the direct relationship with the Mach number is now identified. Again, three terms remain, all depending on M_R to a certain extent. It can be observed that the common denominator is equivalent to the one of the integration constants and to one of the jump conditions for electrons temperature and pressure. This means a singularity is to be expected at $M_R^2 = 2\gamma/(\gamma-1)$, the same limit Mach number as presented in chapter 3.

5.4 Entropy production sign

Unfortunately, the complexity of our parametric expression prevents from performing an analytical study of its sign. Instead, numerical results are processed using known parameters λ and D and right state variables ρ_e^R, ρ_h^R, p_e^R, p^R and M_R from the first case study presented in chapter 4 (table 4.1)

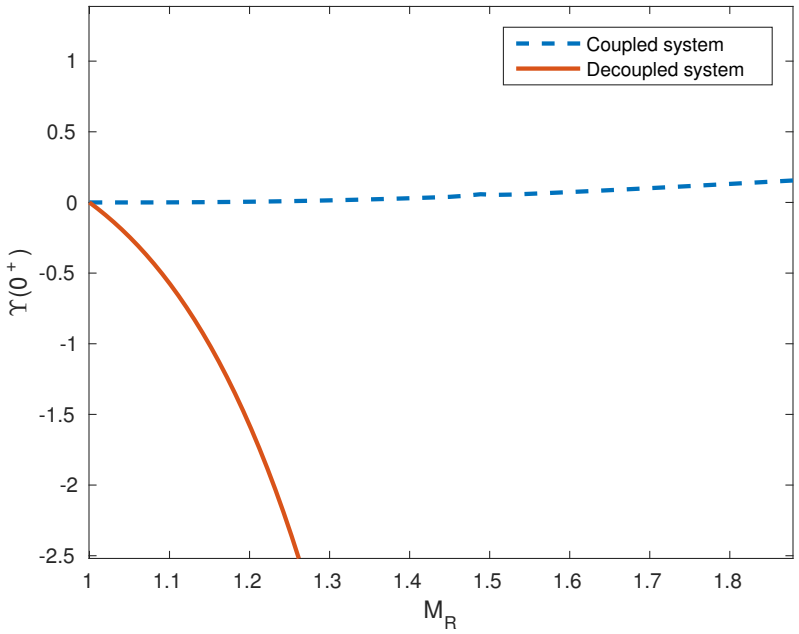

Figure 5.1: Shock entropy production for incoming Mach numbers close to unity.

The obtained results are shown on figures 5.1. It appears that the entropy production of the decoupled case is strictly negative for $M_R > 1$. Two points can then be made, the first one being that the singularity at M_{lim} is not the cause of Υ negative sign as the entropy production is already negative for inferior Mach number. The second remark is essentially that the solution is not physically possible, violating the second law of thermodynamics. Still, though the travelling

wave solution might not reflect reality, it has be shown to be useful in the development of the non-conservative product treatment. Moreover, this was somewhat predicted earlier as "this simplification has no physical justification since the structure of the diffusion is modified" (Wargnier[12]).

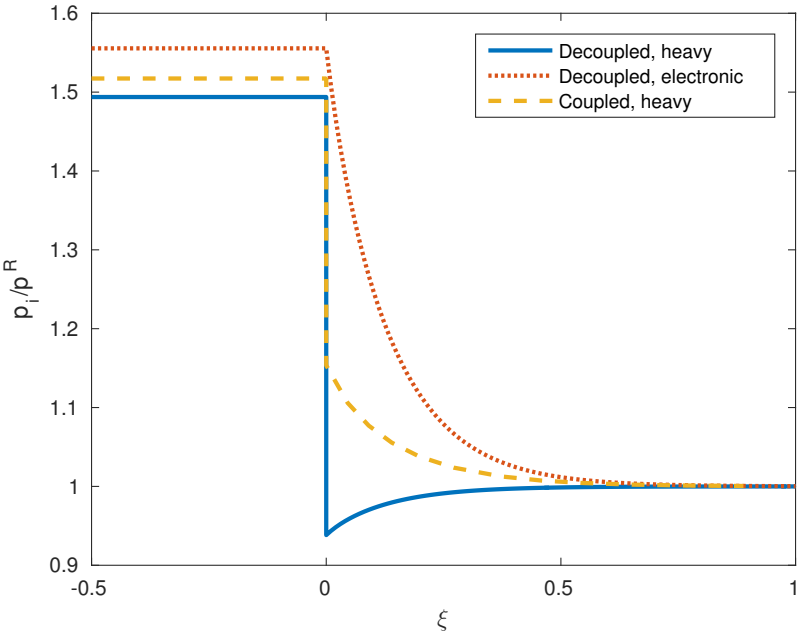

Figure 5.2: Heavy particles pressure for the coupled and decoupled case.

5.5 About heavy particles

One could have noticed that decoupling system 3.2&3.3 has another surprising consequence, which consists of a pressure drop (see 5.4) ahead of the shock. Indeed, considering an electrons pressure increase, a constant global pressure resulting from the Euler system, and recalling

$$p = p_h + p_e,$$

it appears that heavy particles pressure can then only decrease. Again, this is unnatural as reality should appear like the coupled case curve in figure 5.4. Focus in now brought on finding a link between this phenomenon and what was previously observed for entropy that is a negative production. For that purpose, the entropy of heavy particles is derived for both cases. To begin with, a new definition is introduced:

$$s_{h1} = c_v \ln\left(\frac{p_h}{(\gamma-1)(\rho_h^R)^\gamma}\right). \tag{5.10}$$

This directly helps to correlate entropy to the pressure drop. As the heavy particles density is constant in the region of interest ($\xi \geq 0$), it can be stated that the derivatives of p_h and s_h with respect to ξ have a common sign that is positive. Regarding now the negative entropy generation, conservation equation 5.2 is considered in 1D and expressed in terms of ξ as:

$$-\sigma(\rho_h s_h)' + (\rho_h s_h v_h)' = -\frac{1}{T_h}\left(\lambda T_e'' + \frac{5}{2}p_e''\right).$$

Then when isolating the entropy variable,

$$s'_{h2} = \frac{1}{p_h c^R M_R}\left(\lambda T''_e + \frac{5}{2} D p''_e\right). \tag{5.11}$$

If the sign of the ratio is obviously positive, this is not the case for the terms between brackets. Indeed, the electronic temperature has a negative second derivative until a certain inflexion point (see figure 3.1). Therefore, the derivative cannot be considered positive directly. Still, it can be compared to the derivative of s_{h1} using T_e and p_e analytical expressions and developing them as :

$$s'_{h1} = \frac{p'_h}{p_h} = \frac{-\rho_e^R \delta^+ K^{R+} e^{\delta^+ \xi} - \rho_e^R \delta^- K^{R-} e^{\delta^- \xi}}{p_h^R - \rho_e^R (K^{R+} e^{\delta^+ \xi} + K^{R-} e^{\delta^- \xi})}$$

$$s'_{h2} = \frac{\frac{\left[(\frac{5}{2} D \rho_e^R + \lambda(1 - \frac{\delta^+}{\eta^R}))\rho_e^R (\delta^+)^2\right]}{c^R M_R} K^{R+} e^{\delta^+ \xi} + \frac{\left[\frac{5}{2} D \rho_e^R + \lambda(1 - \frac{\delta^-}{\eta^R}))(\delta^-)^2\right]}{c^R M_R} K^{R-} e^{\delta^- \xi}}{p_h^R - \rho_e^R (K^{R+} e^{\delta^+ \xi} + K^{R-} e^{\delta^- \xi})}$$

Beyond the heaviness of these results, it can be noticed that both expressions are similar with only different constants multiplying the exponential at the numerator. A numerical integration of s'_{h2} was performed and illustrated in figure 5.3. The heavy particles entropy from the definition and the one obtained from the conservation equation are almost equal suggesting that the pressure drop and the negative entropy production, from which the curves are derived respectively, are linked and are both indications of an anomaly. However, these observations should be seen as more of a curiosity than a proof of non-validity.

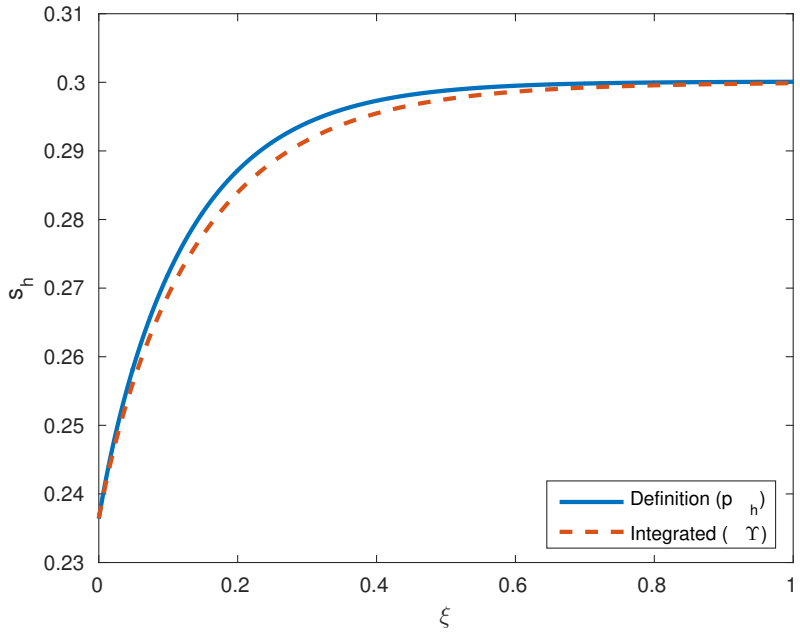

Figure 5.3: Heavy particles entropy evolution ahead of the shock from two different approaches using inputs from case study 4.1.

Chapter 6

Addition of two-temperatures relaxation

The nonconservative product treatment has shown its effectiveness in chapter 4. The developments, used to find the new discretization, neglected the energy exchange term that appears in 2.2. The present chapter focuses on the rehabilitation of the relaxation and to study its impact on the decoupled sub-systems (3.2 & 3.3), its travelling wave solution and the resulting numerical treatment of the nonconservative product.

6.1 Impact on the travelling wave solution

Considering the decoupled system, adding back the 0^{th} exchange term only affects the drift-diffusion subsystem that now reads as :

$$\begin{cases} \partial_t \rho_e + \partial_x \cdot (\rho_e v_h) = \partial_x (D \frac{1}{T_e} \partial_x p_e) \\ \partial_t (\rho_e e_e) + \partial_x (\rho_e e_e v_h) + p_e \partial_x v_h = \partial_x (\lambda \partial_x T_e + \frac{\gamma}{\gamma - 1} D \partial_x p_e) + \Delta E_e^{(0)}. \end{cases} \tag{6.1}$$

An analytical solution for the resulting travelling wave, can no longer be obtained. However, this is not the case for compatibility equations that have the following new expressions:

$$\rho_e(0)[v_h]_{(0)} = \frac{D}{T_e(0)}[p_e']_{(0)}, \quad \text{and} \quad [T_e']_{(0)} = \frac{1}{\lambda} \int_{0^-}^{0^+} \Delta E_e^{(0)} d\xi. \tag{6.2}$$

It appears that the electron temperature derivative is no longer continuous and that its jump at $\xi = 0$ is directly related to the exchange term. The latter will now be discretized in order to use it in the global numerical scheme. First, the exact expression of the term is recalled from equation 2.2 and developed to put forth the unknowns:

$$\Delta E_e^{(0)} = \frac{3}{2} n_e \frac{T_h - T_e}{\tau} = \frac{3\rho_e}{2\tau} \left[\frac{p}{\rho_h} - (\gamma - 1)\rho_e e_e \left(\frac{1}{\rho_h} - \frac{1}{\rho_e} \right) \right].$$

In a discretised sense, this expression becomes:

$$\Omega_{j,2}^n = \frac{3}{2\tau} U_{j,1}^n \left[\frac{p}{\rho_h} - (\gamma - 1) U_{j,2}^n \left(\frac{1}{\rho_h} - \frac{1}{U_{j,1}^n} \right) \right].$$

The $\Omega_{j,2}^n$ contribution in the general scheme, is treated as a source term. The value of τ will influence the weight of the relaxation phenomenon in the electron energy conservation equation. In figure 6.1, the appearance of the resulting electron temperature can be observed for various orders of magnitudes for the time constant τ. For better visualisation, a new test case is used

	p	p_e	ρ_e	ρ_h	v_h	M
State R	1	0.1	0.11111	1	0.2	1.183

Table 6.1: Isothermal upstream test case parameters.

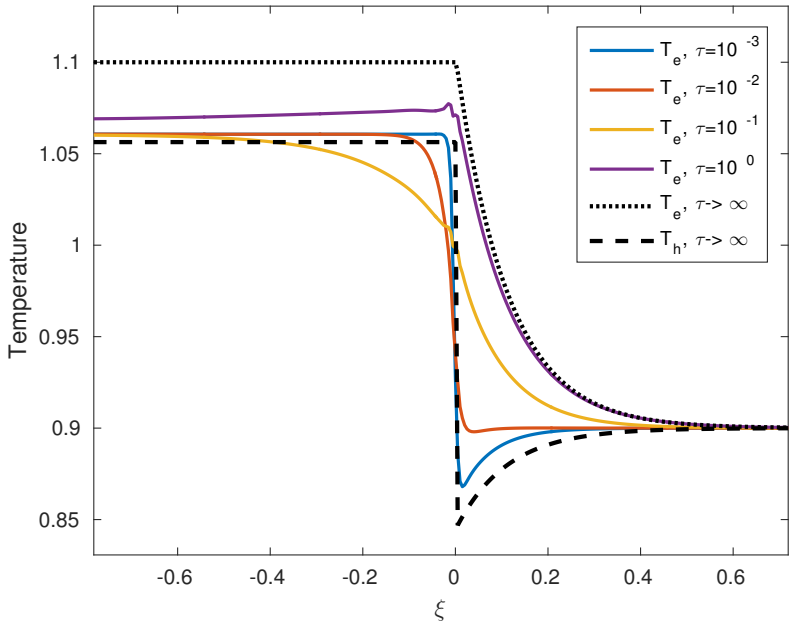

Figure 6.1: Relaxation effect on electronic temperature at t=1.0 for varying τ coefficients with over-resolved standard discretization of the non-conservative product.

with an upstream isothermal input (parameters available in table6.1). Several observations can be made from figure 6.1 beginning with the fact that, for $\tau \to 0$, the electron temperature profile remains closer to heavy particles one, and for $\tau \to \infty$, the electron temperature approaches the case without relaxation. Moreover, a slope discontinuity, for $\tau = 10^{-1}$, appears at $\xi = 0$ as prescribed by the modified compatibility equations. Finally, it is noted that the T_e curves converge towards a temperature slightly higher than T_h in the case without relaxation, as the heavy particles temperature also converges to an equilibrium, but more subtly because of the density ratio between the species.

Additional simulations were achieved, their results being shown on figure 6.2 where time evolves and τ is kept constant. For high time constants τ, meaning small relaxation contributions, it appears that the solution takes longer to converge to a final shape. The figure illustrates the intermediate states of the wave between the initial condition (i.e. the analytical solution of the case without relaxation) and when the simulation was stopped (unfortunately before convergence).

6.2 Impact on the nonconservative product treatment

The impact of relaxation on the development of the treatment of the nonconservative term, will now be shown. The modified general scheme is given as :

$$\begin{cases} U_{j,1}^{n+1} - U_{j,1}^{n} + \frac{\Delta t}{\Delta x}(F_{j+1/2,1}^{n} - F_{j-1/2,1}^{n}) = 0 + \frac{\Delta t}{\Delta x}(G_{j+1/2,1}^{n} - G_{j-1/2,1}^{n}) \\ U_{j,2}^{n+1} - U_{j,2}^{n} + \frac{\Delta t}{\Delta x}(F_{j+1/2,2}^{n} - F_{j-1/2,2}^{n}) = N_{j,2}^{n} + \frac{\Delta t}{\Delta x}(G_{j+1/2,2}^{n} - G_{j-1/2,2}^{n}) + \Omega_{j,2}^{n}, \end{cases} \tag{6.3}$$

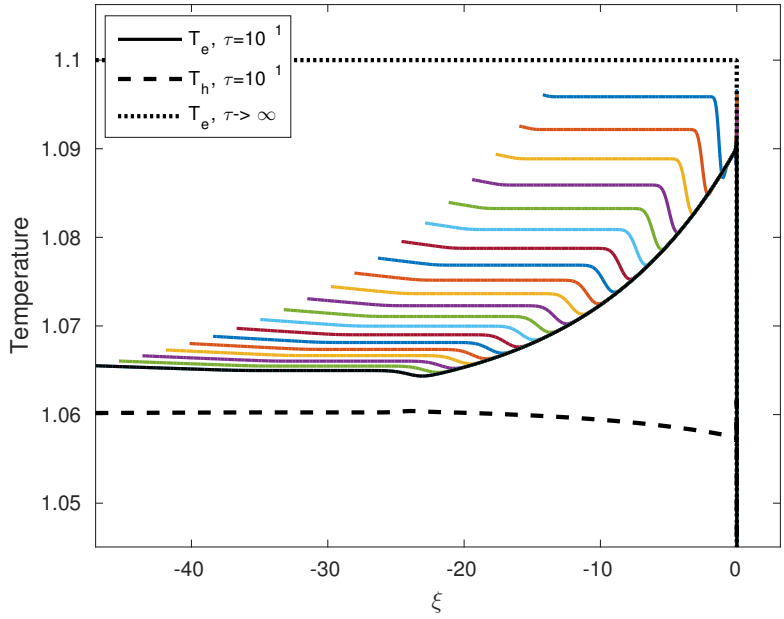

Figure 6.2: Convergence of the downstream electronic temperature along time with $\tau = 10^1$ and with over-resolved standard discretization of the non-conservative product. Simulation stopped at t=50 and intermediate states captured at each integer time.

where $\Omega^n_{j,2}$ is the discretised energy exchange term. To begin with, as the second compatibility equation 6.1 is modified, the diffusive flux difference between the two interfaces of a cell centered at x_j, now reads:

$$G^n_{j+1/2,2} - G^n_{j-1/2,2} = \frac{D\gamma}{\Delta x}(U^n_{j+1,2} - 2U^n_{j,2} + U^n_{j-1,2}) + \Omega^n_{j,2}.$$

Therefore, the coupling between the two coordinates of the diffusive flux is less compact than earlier:

$$G^n_{j\pm1/2,2} = \frac{\gamma}{\gamma-1}T_{e,j\pm1/2}G^n_{j\pm1/2,1} + \frac{\lambda}{\Delta x}(\pm T_{e,j\pm1} \mp T_{e,j}).$$

When applying the same operations to system 6.3 as in section 4.3, a first expression for the discretised non-conservative product is obtained:

$$\begin{aligned} N^n_{j,2} = {} & \frac{\Delta t}{\Delta x}(F^n_{j+1/2,2} - F^n_{j-1/2,2}) - \frac{\gamma}{\gamma-1}T^n_{e,j}\frac{\Delta t}{\Delta x}(F^n_{j+1/2,1} - F^n_{j-1/2,1}) \\ & - \frac{\Delta t}{\Delta x}(H^n_{j+1/2} - H^n_{j-1/2}) - \Delta t\left(1 + \frac{1}{\Delta x^2}\right)\Omega^n_{j,2}, \end{aligned} \tag{6.4}$$

However, although the new compatibility equations are ensured thanks to this expression, this discretization is not consistent with system 6.1. Again, first-order correction terms are needed as the current limit is:

$$\lim_{\Delta x\to 0}\frac{N^n_{j,2}}{\Delta t} = \partial_x(\rho_e e_e v_h) - \frac{\gamma}{\gamma-1}T_e\partial_x(\rho_e v_h) - \Delta E^{(0)}_e + ...\mathcal{O}(\cdot\S^{\in}) \tag{6.5}$$

and the following limit is sought:

$$\lim_{\Delta x\to 0}\frac{N^{n*}_{j,2}}{\Delta t} = -p_e\partial_x v_h. \tag{6.6}$$

Thus, the new correction terms are the old ones from equation 4.3 with the addition of the relaxation term. The final discretization of the nonconservative product is obtained as:

$$\begin{aligned} N_{j,2}^n = & \frac{\Delta t}{\Delta x}(F_{j+1/2,2}^n - F_{j-1/2,2}^n) - \frac{\gamma}{\gamma-1} T_{e,j}^n \frac{\Delta t}{\Delta x}(F_{j+1/2,1}^n - F_{j-1/2,1}^n) \\ & - \frac{\Delta t}{\Delta x}(H_{j+1/2}^n - H_{j-1/2}^n) - \frac{\Delta t}{\Delta x^2}\Omega_{j,2}^n \\ & - \Delta t v_{h,j}^n \frac{U_{j,2}^n - U_{j-1,2}^n}{\Delta x} + \frac{\gamma}{\gamma-1}\Delta t v_{h,j}^n U_{j,1}^n \frac{T_{e,j}^n - T_{e,j-1}^n}{\Delta x}. \end{aligned} \tag{6.7}$$

where a contribution from the energy exchange term now appears and is second-order. However, the python code that was provided and that retrieves the results of chapter 4, doesn't use the second order terms. Adding the second order relaxation contribution actually causes the simulation to crash. Therefore, the discretization of the nonconservative product will be kept as it was.

6.3 Results for an under-resolved case

The effectiveness of the numerical treatment of the nonconservative product will now be assessed in the case of relaxation, comparing its performances with the standard discretisation on a fine and a coarse mesh, as done in chapter 4. In order to obtain a first glance of the impact of the energy exchange on both schemes, the difference between their results was computed and the time constant τ was given various orders of magnitude. Figure 6.3 shows that the difference between the two schemes declines when increasing the relaxation contribution, especially for the under-resolved case whose maximum reaches approximately the same value as the one of the over-resolved case, though it is twice as big as without relaxation. Note that, again, the results of this section use the same test case as in chapter 4 (table 4.1).

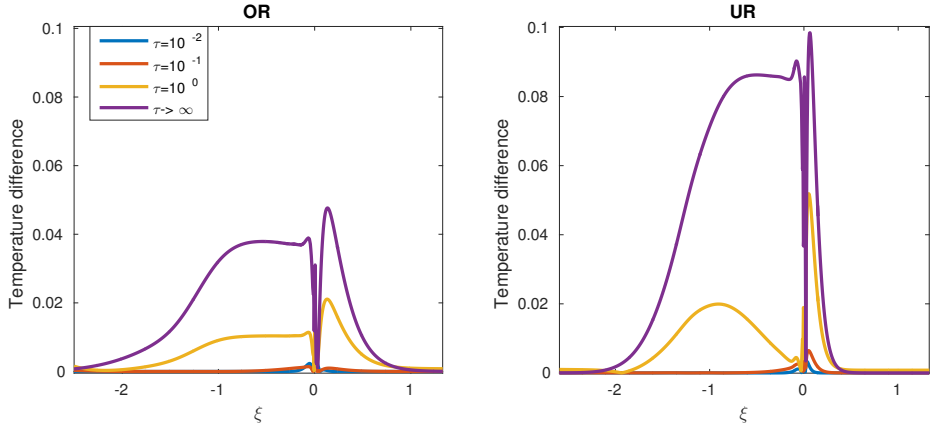

Figure 6.3: Electron temperature difference between the standard and new discretization of the nonconservative product for varying τ in over-resolved (OR) and under-resolved case (UR).

Moreover, one can refer to the results of Wargnier[12] on figure 4.5. However, to obtain the error of numerical results requires a reference that cannot be analytical in the relaxation case. In that purpose, a simulation was ran with five times more volumes, i.e. N=10,000, using the standard scheme as it should be the most consistent for $\Delta x \to 0$. Then, computing the L_2-norm of such an error, the curves in figure 6.4 were obtained. The time constant value $\tau = 10^{-1}$ was chosen in such a way that the solution would converge at the simulation time $t_f = 1$. From there, it appears that the new numerical treatment keeps on performing better than the standard discretization. Both find their error reduced by around an order of magnitude, allowing the possibility to use a coarser mesh with the standard discretization as the error would not overtake the one of the new treatment in an over-resolved case. As a conclusion, relaxation has a positive impact on both schemes though the new numerical treatment of the nonconservative term remains more effective.

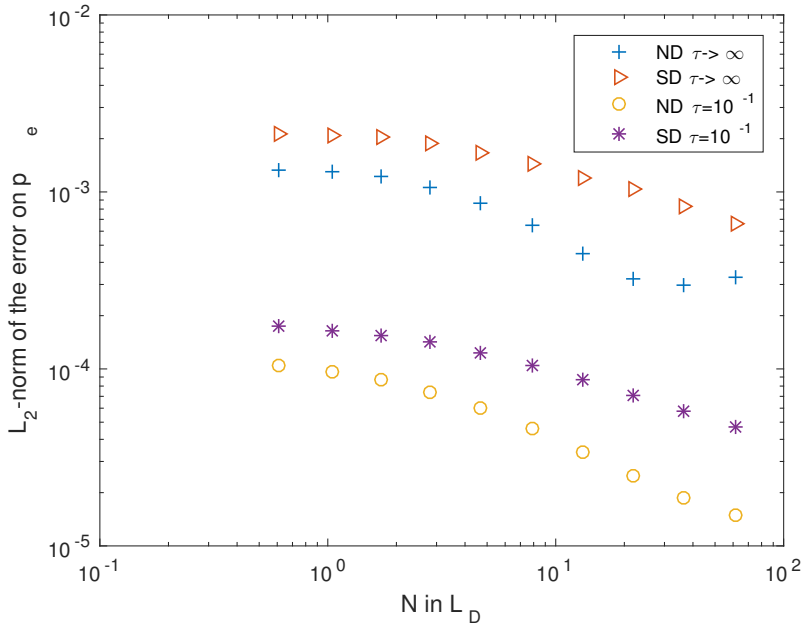

Figure 6.4: L_2-norm of the error with respect to the number of nodes in L_D of the standard (SD) and new (ND) discretizations of the nonconservative product with and without relaxation ($\tau = 10^{-1}$) at t=1.

General Conclusion

The multi-component model proposed by Graille&al [1] and presented in chapter 2 has the advantage of being rigorously derived from kinetics theory while, still, it is "able to capture most of the multi-fluid phenomena" (Wargnier[12]). However, it introduces an issue that is the presence of a nonconservative product, preventing one to use the usual Riemann problem solving schemes for the whole hyperbolic part of the system, in a finite volume method. Among various approaches proposed in the literature, one decouples the system by removing diffusive terms in the total energy equation, leaving a classic Euler system as well as a drift-diffusion system for which an analytical travelling wave solution can be obtained. The numerical treatment of the nonconservative product, proposed by Wargnier[12], benefits from such a method and fixes the issue of an artificial jump appearance in coarse meshes with respect to the diffusion length scale when using a standard discretization.

The fist part of the contribution brought by this work, focused on the physical validity of the decoupling approach with respect to the second principle of thermodynamics. An expression of entropy production was derived with respect to the incoming Mach number for both the coupled and decoupled cases. It appeared that the quantity of the latter is negative for the upstream region and for incoming Mach numbers greater than unity, meaning that such a result is not the cause of the validity limitation of the solution approach to Mach numbers close to unity, but still violates reality. Moreover, an anomaly, consisting of a drop of the heavy particles upstream pressure (and temperature) was found. Finally, its link with the negative entropy generation was put in evidence. However, although the undoubted negative impact of the decoupling of the model on physical validity was proved, it can be stated than such an approach remains attractive thanks to its elegant analytical solution and jump conditions close to the ones of the coupled case. It also allowed to develop a new numerical treatment of the nonconservative product, whose benefits had been shown (see 4.5).

The second contribution was the rehabilitation of the relaxation phenomenon through the addition of a energy exchange term in the electron energy conservation equation. Its impact on the compatibility equations as well as on the behaviour of the solution for various orders of magnitude of relaxation time constants was presented. Regarding the new discretization of the nonconservative term, it was shown to also change with the addition of relaxation. Its new performances were assessed at various resolutions and it appears that the treatment remains more advantageous than the standard discretization, though it might no be necessary anymore. Indeed, more generally, relaxation greatly improves the performance of both schemes.

This last contribution is part of a process that consists of applying the strategy used to develop the numerical treatment of the nonconservative product, to more complex versions of the model developed by Graille&al[1]. A first step would be to apply such a method to the coupled system 3.1, therefore benefiting from five compatibility equations, as suggested by Wargnier[12]. Then, other terms could be added such as the ones accounting from the chemistry and the electromagnetism of the problem. The benefits of this scheme strategy still need to be proven for such cases.

Appendix A

Resolution of the coupled model

Although it cannot be applied in a finite volume method or extended to more dimensions, a relatively quick method, introduced in Wargnier[12], exists to solve the coupled system 3.1. The wave structure (shown in figure A.1 that is expected would be :

- A constant down stream state for the electronic variables, preceded by a regularization up to the freestream state.
- Also a constant down stream state for the heavy particles variables and the total energy, but with a jump at the discontinuity before again regularising.

Development : One can recall that momentum and total pressure are conserved, meaning mass and pressure can always be expressed as functions of the fluid velocity:

$$\begin{aligned} \rho_h u_h = k_1, \quad k_1 \in \mathbb{R} \qquad &\rightarrow \quad \rho_h = \alpha(v_h) \\ m_h v_h + p = k_2, \quad k_2 \in \mathbb{R} \qquad &\rightarrow \quad p = \beta(v_h) \end{aligned}$$

where $m_h = \rho_h u_h$ is the conserved momentum,$u_h = v_h - \sigma$ the velocity expressed in the laboratory referential and σ is the shock speed. Now, expressing the coupled system 3.1 in the wave referential, with $\xi = x - \sigma t$ as the spatial variable, one gets these three following ODEs as two first equation are equivalent to the conservation of the aforementioned quantities. Hence :

$$\begin{cases} (\mathcal{E} u_h + p v_h)' = \lambda T_e'' + \frac{\gamma}{\gamma-1} D p_e'' \\ (\rho_e u_h)' = (D \frac{1}{T_e} p_e')' \\ \frac{1}{\gamma-1}(p_e u_h)' + p_e v_h' = \lambda T_e'' + \frac{\gamma}{\gamma-1} D p_e'. \end{cases} \tag{A.1}$$

A new quantities that can be seen as an extended momentum also accounting for thermal velocities, is introduced as : $\Gamma(v_h)\mathcal{E} u_h + p v_h$. Now, when integrating the system from $\xi = 0^+$ to $\xi^* > 0$, one obtains:

$$\begin{cases} \Gamma(v_h(\xi^*)) - \Gamma(v_h(0^+)) = \lambda T_e'(\xi^*) + \frac{\gamma}{\gamma-1} D p_e'(\xi^*) - \frac{\gamma}{\gamma-1} D p_e'(0^+) \\ \rho_e u_h(\xi^*) - \rho_e u_h(0) = D \frac{1}{T_e} p_e'(\xi^*) - D \frac{1}{T_e(0^+)} p_e'(0^+) \\ \frac{1}{\gamma-1}(p_e v_h)' + \frac{1}{\gamma-1} u_h p_e' = \Gamma(v_h)' = \partial_{v_h}\Gamma(v_h) v_h', \end{cases} \tag{A.2}$$

where the first line was used to re-express the third one. The system can now be arranged into an equation of matrices as :

$$\begin{pmatrix} \lambda & \frac{\gamma}{\gamma-1} D & 0 \\ 0 & D & 0 \\ 0 & \frac{u_h}{\gamma-1} & \partial_{v_h}\Gamma(v_h) - \frac{1}{\gamma-1} p_e \end{pmatrix} \begin{pmatrix} T_e \\ p_e \\ v_h \end{pmatrix}' = \begin{pmatrix} \Gamma(v_h(\xi^*)) - \Gamma(v_h(0^+)) + \frac{\gamma}{\gamma-1} D p_e'(0^+) \\ p_e u_h(\xi^*) - \rho_e(0^+) T_e(\xi^*) u_h(0^+) + \frac{D T_e(\xi^*)}{T_e(0^+)} p_e'(0^+) \\ 0 \end{pmatrix}$$

This system of ordinary differential equation can simply be found by first finding the invert of the square matrix and then multiplying it by the right-hand side vector, giving a set of decoupled ODEs. These can then be solved using any integration scheme.

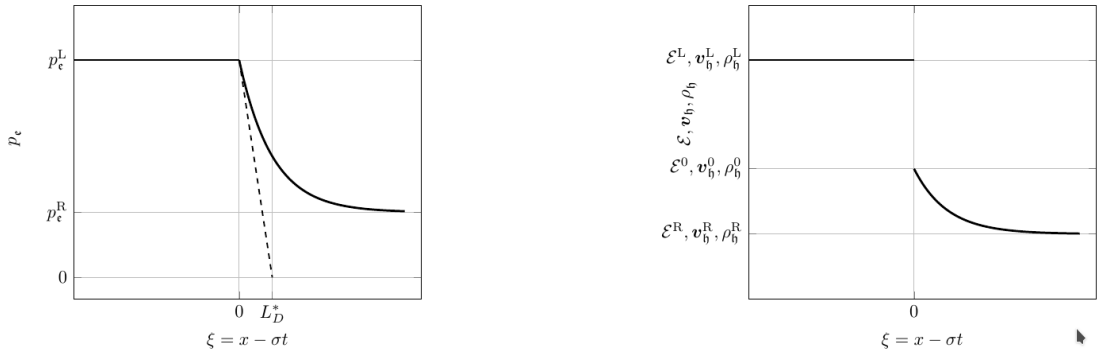

Figure A.1: Structure of the solution of the coupled case from Wargnier.

Initial value : Solving the system requires to know the value of the unknowns at $\xi \to 0^+$. This is not easy to find if one only knows the free stream parameters. Indeed, the values at the discontinuity are closely related to the downstream (Left) state that is unknown. This issue can be fixed using shooting methods where p^L and p_e^L are converged towards a final value. The jump conditions of the decoupling approach are used as a first guess. Such method was used to obtain the pressure jump condition as a function of the incoming Mach number in 3.3.

References

[1] T. E. Magin B. Graille and M. Massot. "Kinetic theory of plasmas: translational energy". In: *Mathematical Models and Methods in Applied Sciences* 19.4 (2009), pp. 527–599.

[2] S.I. Braginskii. "Transport Processes in a Plasma". In: *Reviews of Plasma Physics* 1 (1965), p. 205.

[3] G. V. Candler and R. W. Maccormack. "Computation of weakly ionized hypersonic flows in thermochemical nonequilibrium". In: *Journal of Thermophysics and Heat Transfer* (1991), pp. 266–273.

[4] C. Chalons and F. Coquel. " A new comment on the computation of non-conservative products using roe-type path conservative schemes". In: *Journal of Computational Physics* 335 (2017), pp. 592–604.

[5] F. Coquel and C. Marmignon. "A roe-type linearization for the euler equations for weak-lyionized multi-component and multi-temperature gas". In: *Computational Fluid Dynamics Conference* 12th (1995).

[6] B. Graille S. Faure. "Problème de Riemann — Solveur de Godunov". In: ().

[7] P. L. Floch G. D. Maso and F. Murat. *Definition and weak stability of nonconservative products*. J. Math. Pures et Appl, 1995, pp. 480–550.

[8] A. Klomfass and S. Muller. "A quasi-onedimensional approach for hypersonic stagnation-point flows". In: *Lehr- Und Forschungsgebiet Fur Mechanik* (2007).

[9] R. J. LeVeque. "Finite Volume Methods for Hyperbolic Problems". In: (2002).

[10] *Multi-Scale Models and Computational Methods for Aerothermodynamics*. Ph.D. thesis, Ecole Central Paris, 2014.

[11] J. Scoggins. *Développement de méthodes numériques et étude des phénomènes couplés d'écoulement, de rayonnement, et d'ablation dans les problèmes d'entrée atmosphérique*. Université Paris-Saclay, 2017, pp. 1–45.

[12] Q. Wargnier. *Mathematical modeling and simulation of non-equilibrium plasmas: application to magnetic reconnection in the Sun atmosphere*. Université Paris-Saclay, 2019.

[13] Y. B. Zeldovich and Y. P. Raizer. *Physics of Shock Waves and High-Temperature Hydrodynamic Phenomena*. Academic Press, 1967. ISBN: 978-0-12-395672-9.

UNIVERSITÉ CATHOLIQUE DE LOUVAIN
École polytechnique de Louvain
Rue Archimède, 1 bte L6.11.01, 1348 Louvain-la-Neuve, Belgique | **www.uclouvain.be/epl**